



Studies on Atmospheric Depositions over the Ocean

平木, 隆年

(Degree)

博士 (工学)

(Date of Degree)

2003-09-30

(Date of Publication)

2010-07-16

(Resource Type)

doctoral thesis

(Report Number)

乙0004

(URL)

<https://hdl.handle.net/20.500.14094/DS200004>

※ 当コンテンツは神戸大学の学術成果です。無断複製・不正使用等を禁じます。著作権法で認められている範囲内で、適切にご利用ください。



Kobe University of Mercantile Marine

Doctoral Dissertation

**STUDIES ON ATMOSPHERIC DEPOSITIONS
OVER THE OCEAN**

June 2003

Takatoshi Hiraki

P r e f a c e

Anthropogenic atmospheric depositions have changed with the time. The long-range transported air pollution has been a major concern in our atmospheric environment since the late 1960s. It was proved that the increase of atmospheric depositions in remote places in Europe and U.S.A. was resulted from the long-range transportation of air pollutants. It is an important environmental problem.

The sea surface covers about 70% of the earth surface, and a large amount of air pollutants is transported from land to the ocean. The atmospheric deposition over the ocean is one of the major sink of long-range transported anthropogenic air pollutants. On the other hand, the sea surface also plays as a generation source of salt nuclei which functions as condensation nuclei of micro cloud droplets. The exchange of salt nuclei between the ocean and the atmosphere is an important mechanism in the earth environment. But, there are few opportunities to investigate the atmospheric deposition over the ocean. Because, it is quite difficult and almost impossible to set many rain gauges everywhere to deploy widely the precipitation measurement in wide seas.

The installation of rain sampling devices in the whole ocean is not so easy as on land. Therefore, for the precipitation measurement over the ocean to use ocean going vessels is expected although the measuring method of precipitation on board has not been established yet. The accurate precipitation measurement on board is very difficult because the wind flow over a ship is distorted due to her hull, and the measurement on board includes a big error because of this distorted flow on board. At first, this research is aimed and focused to evaluate the precipitation measurement under strong wind

conditions higher than 10m/s for the purpose of developing the measuring method of the atmospheric depositions over the ocean.

Sea-salt compositions are found in atmospheric depositions as a major component all over the world. It is quite important to evaluate the constituents of sea salt and estimate the portion of sea-salt in the atmospheric deposition. There is some ions related to the acidity of the atmospheric depositions such as Cl^- , NO_3^- , SO_4^{2-} . These ions are known as anthropogenic pollutant constituents in the field of atmospheric environmental science. However, Cl^- and SO_4^{2-} are also the main components of seawater. It is important to distinguish anthropogenic pollutant constituents (e.g., non-sea-salt SO_4^{2-} , hereafter referred to nss- SO_4^{2-}) from natural constituents (e.g., SO_4^{2-}). The chemical composition of sea-salt particles generated by bubble breaking on the surface is different from that of bulk seawater. Many anomalous ion ratios of marine constituents of atmospheric aerosols and rainwater are resulted from the ion enrichment in aerosols scattered by bursting bubbles. We evaluated the chemical composition of sea-salt particles over the Pacific Ocean.

The influence of anthropogenic pollutant constituents in remote areas is very slight so that it is usually so hard to detect it. However, in the areas where the polluted air mass flows in, the composition of atmospheric depositions is changing steadily. In these areas, many anthropogenic pollutant constituents are oxidized by atmospheric ozone. In recent years, the concentration increase of tropospheric ozone has been pointed out. The increase of tropospheric ozone is a remarkable phenomenon in atmospheric chemistry and the dissipation process of atmospheric pollutant constituents.

Stratospheric ozone is essential for life on the earth because it strongly absorbs harmful ultraviolet radiation. Ozone attracted attention so strongly and widely in the last

century. The first incident concerned with ozone happened in the late 1940's. A remarkable air pollution phenomenon began to impact in the district of Los Angeles, U.S.A. The ambient air contained strongly oxidizing, eye-watering and plants-killing pollutants. The second incident pointed out the importance of ozone happened in the mid-1970s. It was recognized that CFCs were a potential threat to the decomposition of stratospheric ozone. In 1982 and 1985, the discovery of the Antarctic Ozone Hole was a dramatic confirmation of the role of CFCs in the ozone depletion.

The Vienna Convention for the Protection of Ozone Layer agreed in March, 1985 on the need to control the emission of CFCs and other chlorine-containing substances. This was followed by the Montreal Protocol in September, 1987. The third incident was related to the Greenhouse effect pointed out in the past decade. The global increase of ozone has also been documented recently although the geographic distribution and the temporal change are complicated. The numerical model showed that significant radiative effects resulted in the change in the ozone concentration in the upper troposphere since the pre-industrial time.

The stratosphere-troposphere vertical mixing plays an important role in atmospheric environmental issues. On the other hand, the horizontal mixing along isentropic surfaces in the lower stratosphere and the troposphere can be faster than the vertical mixing between both atmospheric layers over the world. This mechanism contributes to the maximum ozone concentration in spring. The geographic distribution and the seasonal variation of tropospheric ozone will reveal the formation and the transportation of ozone and the reaction of ozone with anthropogenic pollutants.

Contents

Preface	i
Chapter 1 Improvement of Atmospheric Deposition Sampler on Board	1
1.1 Introduction	1
1.2 Design of Atmospheric Deposition Sampler	3
1.2.1 Sampler Design for Measurement in Remote Forest	3
1.2.2 Sampler Design for Measurement on Board	6
1.3 Result and Discussion	8
1.3.1 Accuracy of Filtrating Bulk Sampler	8
1.3.2 Evaluation of Opening Face Angle	9
1.3.3 Collection Efficiency of Rainfall	11
1.3.4 Comparison of Collection Efficiency	14
1.4 Conclusion	16
Chapter 2 Measurement of Atmospheric Deposition over the Western Pacific Equatorial Ocean	19
2.1 Introduction	19
2.2 Observation and Analytical Method	20
2.3 Result and Discussion	24
2.3.1 Overview of Atmospheric Deposition	24
2.3.2 Wet and Dry Depositions	28

2.3.3 Chemical Constituent of Atmospheric Deposition	31
2.3.4 Acidity of Deposition	35
3.3.5 Generation of Sea-Salt Particle	38
2.4 Conclusion	39

Chapter 3 Characteristics of Atmospheric Deposition over the North Pacific

Ocean	43
3.1 Introduction	43
3.2 Observation and Analytical Method	44
3.3 Chemical Analysis	46
3.3.1 Evaluation of Analytical Quality	46
3.3.2 Sea-Salt Constituent	47
3.3.3 Origin of NO_3^-	50
3.3.4 Chemical Characteristics	52
3.4 Conclusion	55

Chapter 4 Seasonal Variation of Atmospheric Ozone Concentration over the

Western Pacific Ocean	61
4.1 Introduction	61
4.2 Observation and Analytical Method	63
4.3 Result and Discussion	66
4.3.1 General Feature of Ozone Concentration	66
4.3.2 Meridional Distribution of Ozone Concentration	68
4.3.3 Seasonal Variation of Ozone Concentration	70

4.3.4 Seasonal Characteristics of Meteorological Elements and Ozone Concentration	72
4.3.5 Air Mass Trajectory Analysis	74
4.4 Conclusion	80
Chapter 5 Conclusion	85
Acknowledgments	89

Chapter 1

Improvement of Atmospheric Deposition Sampler on Board

1.1 Introduction

Long-range transferred air pollution has been a major concern since the late 1960s. The first survey on rainwater in Japan was started in Tokyo and Kobe in 1935. Since then, nearly 4,000 reports on so-called acid rain have been published by about five hundred research groups in Japan (Tamaki⁽¹⁾). The annual mean pH of rainwater in Japan, as determined by the worldwide standard method using a wet/dry sampler, was reported about 4.6 (Tamaki and Hiraki⁽²⁾).

The main portion of pollutants in the oceanic area is deposited from the atmosphere. But the amount of the atmospheric deposition over the ocean has not been clarified yet. There are many difficulties to measure the atmospheric depositions in the sea. It is quite difficult and almost impossible to set rain gauges everywhere to deploy widely the precipitation measurement in many seas. The installation of the sampling devices in the whole ocean is not so easy as on land. Therefore, to use ocean going vessels is expected for the precipitation measurement. In the weather report in the sea, the observational data from merchant vessels cruising in various oceans in the world are so important. However, the precipitation data are not contained in the weather

observational items on board because the precipitation can not be measured on board due to strong relative winds (e.g., Hall and Upton⁽³⁾).

Also in the precipitation measurement on land, the measurement error due to strong winds is an important subject. When measuring snowfall, the measurement error is remarkable and many researches have been reported. Rasmussen *et al.*⁽⁴⁾ studied the precise snowfall measurement for the deicing decision of an airplane. They compared the value of the snow pan measured every 15 minutes manually with the values of ordinal snow gauges equipped with various windshields. They found out that the mean value of the snow gauge with the best windshield was not different so much from the mean of the snow pan. The difference among them was only 5% of the mean of the snow pan. However, most of the data were scattered widely and in the range of 30% of the mean of the snow pan. Recently, they have developed the disk type of the hotplate snow gauge, and found that the precise snow measurements could be estimated by using the correction coefficient under wind velocity of 9m/s although the collection efficiency fell down to 20% at high wind velocity of 10m/sec⁽⁵⁾. Although under the condition less than 9m/sec, the outstanding performance was shown by the original algorithm of the collection efficiency and wind velocity.

This research is aimed at and focused on the evaluation of the precipitation measurement under strong wind conditions higher than 10m/s for the purpose of developing the measuring method of the atmospheric depositions over the ocean.

1.2 Design of Atmospheric Deposition Sampler

1.2.1 Sampler Design for Measurement in Remote Forest

The optimal atmospheric deposition sampler for the on-board observation was developed. The sampler was improved on the basis of a filtrating bulk sampler used widely by the atmospheric deposition measurement in Japan for the simple and easy installation and handling in the field observation. This sampler also fits use in the forest of a remote place, and investigated was the measurement accuracy in the field of a forest area.

The experiments were carried out at Kobe Municipal Arboretum (ca. 370 m above sea level) from Sept. 1991 to Mar. 1995, and the routine measurement has been still continued now. The arboretum has many kinds of trees in a 142 ha site, the largest in Japan, and is located in Kobe city, Hyogo prefecture, central Japan. The surrounding areas do not have major sources of air pollutants, but the arboretum is located in the northern part of Kobe city, with over 1,400,000 population, and is indirectly affected by air pollution from the urban area. The main forest used in the experiments was *Chamaecyparis obtusa*, and *Cryptomeria japonica*- and *Quercus serrata*- forest were also used for several experiments. All the forests were planted over fifty years ago.

A filtrating bulk sampler, widely used in Japan due to its convenience for acid deposition monitoring, was modified for rainfall- and throughfall-sampling in the forest area. The main improvements were as follows. The sampler was made compact, fixed at 1.7 m above ground level using a stainless steel pole, and shaded from sunlight by silvery paint and a black vinyl cover (Figure 1.1). Two kinds of the filters ($0.8 \mu\text{m}$,

47mm ϕ Millipore AAWG and Nuclepore polycarbonate) were used for the separation of insoluble components. Three samplers were set in different locations near the *Cryptomeria japonica* forest to investigate the dependence of the rainfall data on the sampling point.

The type of the sampler used for rainfall sampling was also used for a throughfall experiment. Two samplers were set in the *Chamaecyparis obtusa* forest, within 2 m apart. One was a conventional rainfall sampler and the other was slightly modified as follows: a conical nylon net was placed inside a polyethylene funnel to prevent the disturbance of rainwater flow by leaves. The rainwater amount and concentrations of chemical components obtained by these two samplers were compared each other.

Rainfall and throughfall were collected on an event basis as a general rule, and pH, electric conductivity, SO_4^{2-} , NO_3^- , Cl^- , NH_4^+ , Ca^{2+} , Mg^{2+} , K^+ , and Na^+ in the rainwater were measured within one week after sampling by the method reported previously (Japan Environment Agency⁽⁶⁾).

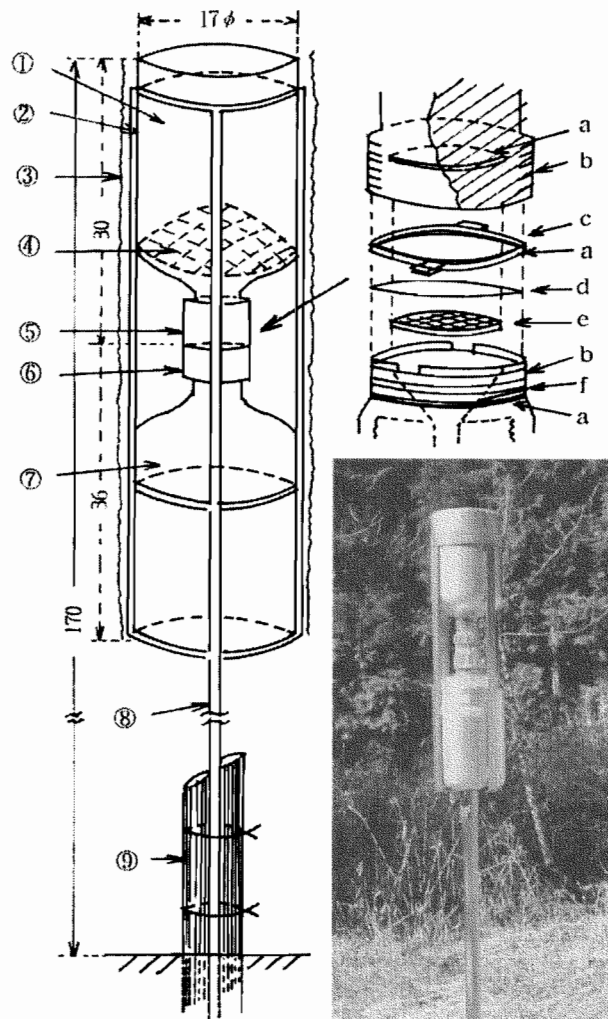


Figure 1.1 Rainfall- and throughfall- sampler.

(① polyethylene funnel, ② light shade: coating of silvery paint, ③ light shade :black vinyl cover, ④ nylon net, ⑤ filter holder(filter:0.8 μ m, 47 mm ϕ , Nuclepore polycarbonate PC memb. or Millipore AAWP), ⑥ air duct, ⑦ polyethylene tank (100 L), ⑧ stainless steel pole, ⑨ stake, a:o-ring, b:screw, c:filter cover, d:filter, e:filter plate, f:air duct.

1.2.2 Sampler Design for Measurement on Board

The samples were collected once a day during cruises in the Western Pacific Ocean and a part of the Indian Ocean from August to September in 1993 and 1994 by three kinds of precipitation collectors. The collectors were installed on the top deck of the P/V Orient Venus (gross tonnage:22,000 t, overall length:170 m, width:24 m, ship's speed:21 knots), at the height of about 22 m above the sea surface. Three kinds of precipitation collectors were shown in Figure 1.2. Type I collector was manufactured with reference to the inverted Frisbee type of the deposit gauge currently developed by Hall and Upton⁽³⁾. Moreover, it is designed based on the same idea as the hotplate type snow gauge of Rasmussen *et al.*⁽⁵⁾. It does not require a wind shield, because the hotplate has a minimal effect on the airflow around it due to its aerodynamic shape.

Type II collector was a bulk sampler that we usually use in the field investigation as described above. Although this is a little smaller than NILU-type bulk collectors used widely in Europe, its form and quality are similar to that. Type III is made by slanting the opening of the upper funnel of Type II collector to catch the precipitation more effectively under strong against wind conditions. These consist of a polyethylene funnel and bottle. Their diameter and length are 165 and 215mm, respectively. A membrane filter (AAWP47, 0.8 μ m pore size) is placed at the bottom of the upper funnel to avoid collecting local debris in the air and rain.

Each collector was installed in the port and starboard sides near the center. When there was the crosswind, the difference were found in the precipitation of both sides. In order to evaluate the systematic error included as a result of observation, the type III collector was installed in both sides.

In this research, rain and atmospheric depositions collected with each equipment were examined in order to investigate the collection efficiency of the precipitation and the amount of atmospheric depositions. When it rained during sampling periods, rain water and depositions were collected as a bulk sample. When it did not rain during sampling periods, depositions captured inside the collector was washed down with 100ml of distilled water and washed water was collected as a dry deposition sample.

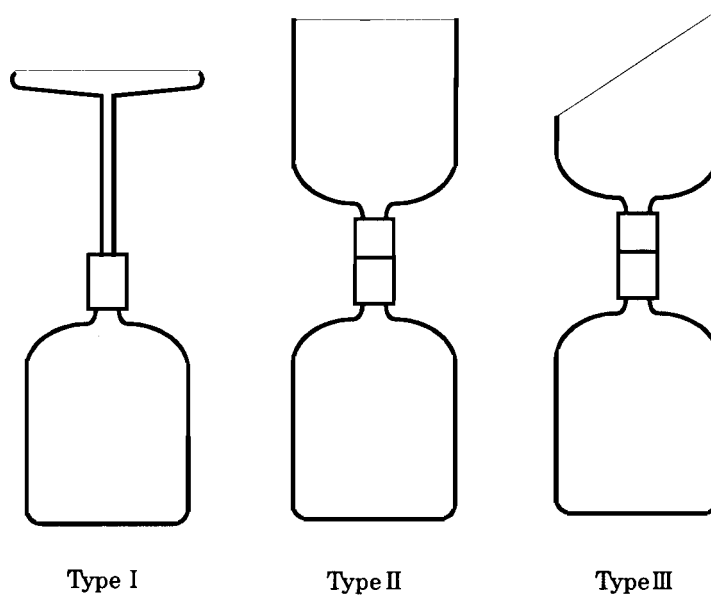


Figure 1.2 Three types of atmospheric deposition collectors.

The height and diameter of the funnel and bottle are 165 and 215mm, respectively. The volume of the storage bottle is 5 liter.

1.3 Results and Discussion

1.3.1 Accuracy of Filtrating Bulk Sampler

For long-term monitoring in a forest, the use of a filtrating bulk sampler was examined. This type of sampler is inexpensive and can prevent the change of sample quality. The results of measurements showed that the mean rainfall amount collected by the modified filtrating bulk sampler was about 3% smaller than that collected by the wet/dry sampler in the forest, and that the pH value, and NH_4^+ , as well as NO_3^- concentrations did not change during the sampling period of 2 weeks. The sampler has been used in two forests for long-term monitoring more than eight years without any problems.

The difference among the sampling amounts at three points within 330 m distance and 45 m height was less than 8% of the mean. The choice of a sampling point appears to be mostly negligible, if there is no significant obstruction by trees. Comparing the data obtained by an automatic acid rain analyzer(Kimoto AR107SNA), set 2 km away from the edge of the forest, with the data in the forests, the rainfall amount was slightly lower and the pH value was slightly higher than those by the automatic acid rain analyzer. These difference is, however, slight, so these results confirmed that the modified sampler is suitable for monitoring in a forest.

The effectiveness of a net for protection against fallen leaves was examined. The rainfall amount obtained by the sampler without the net was larger than that with the net, but the difference was less than 1% of that without the net. The pH value obtained by the sampler with the net was slightly higher than that without a net, but the difference in

pH and ion concentration was vanishingly small. These results showed that the collection efficiency was not reduced and the chemical properties of rainwater were not affected by the net. Accordingly, the use of a nylon net is recommended not only for the throughfall sampling but also for the rainfall one. Usually, for the filtrating bulk sampler, 0.8 μ m, 47mm ϕ Millipore AAWG filter is used, but this filter is melted easily by organic compounds from insects. Therefore, in a forest area, 0.8 μ m, 47mm ϕ Nucleopore polycarbonate, in spite of its difficulty in handling, is desirable for the protection of samples. In this study, two types of filters were used, and no differences in the concentrations of chemical components were observed.

1.3.2 Evaluation of Opening Face Angle

When cruising, the precipitation collector on board also has relative wind speed too. Therefore, when the collection efficiency of Type III collector is evaluated, horizontal deposition velocity should be also taken into consideration.

The relation between the slant angle of the opening and the collection efficiency is shown in Figure 1.3 with the ratio of horizontal wind speed (v) to deposition velocity (V_d). The collection efficiency was calculated assuming that the virtual collection opening does not produce the turbulent flow aerodynamically. The line at the ratio of zero shows the collection efficiency when the relative wind velocity to the ship is zero. In this case, the collection efficiency is 100% and constant, irrespective of the form of the precipitation collector.

As the deposition velocity of rain is prescribed by the size of raindrops, the deposition velocity V_d of a raindrop with 1mm diameter is about 6.5m/sec. Since the relative wind velocity in this investigation was 12m/sec, the ratio of horizontal speed

ratio to deposition velocity is 1.85. The collection efficiency, when the slant angle of the opening is 45 degrees, becomes about 280% as shown in Figure 1.3.

The collection efficiency of the precipitation collector of Type III is shown in Table 1.1, according to the size of raindrops and relative wind velocity observed in this investigation.

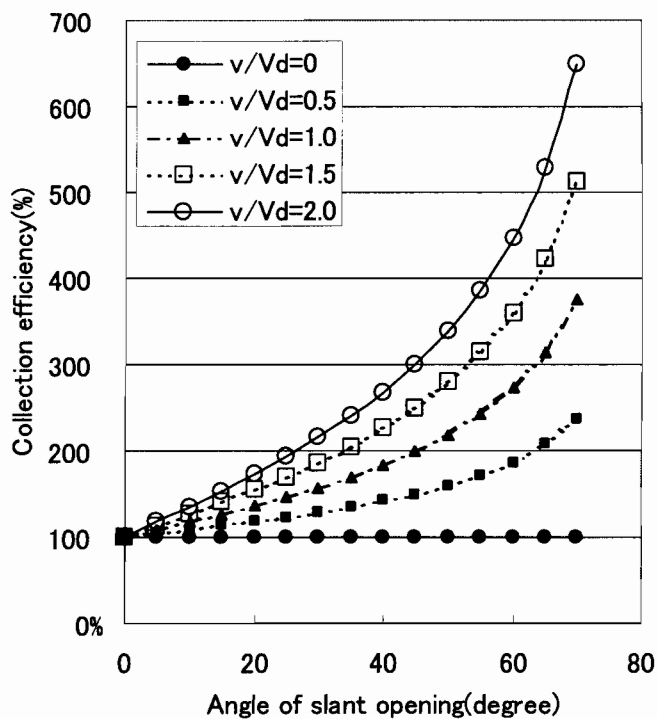


Figure 1.3 Collection efficiency of Type III collector.

v:wind velocity on board, Vd:deposition velocity

Table 1.1 Collection efficiency of Type III collector.

radius of rain drop (mm)	wind velocity (m/s)			
	5	10	15	20
0.1	804%	1508%	2213%	2917%
1.0	177%	254%	331%	408%
2.0	157%	213%	270%	327%
2.9	155%	209%	264%	318%

1.3.3 Collection Efficiency of Rainfall

In order to investigate the deviation of the precipitation distribution on the deck, two sets of the measurements by Type III collector were compared each other. They were installed in the starboard and the port side of the deck. As summarized in Table 1.2, there are few deviations of the precipitation amount and ion species depositions, and the value of standard deviation is also small. Therefore, there were no deviations of the precipitation distributions by the different places on the deck.

The numbers of the precipitation samples collected with Type I, II, and III collectors in both years of 1993 and 1994 were 10, 13, and 15, respectively. Therefore, the collection probability of Type III was higher than Type I and II. Moreover, the measured daily precipitations of Type I, II, and III collectors were 0-10.3mm, 0.0-32.7mm, and 0.1-87.9mm, respectively. Type III could collect the precipitation more

than the others. It was concluded that the collection efficiency of Type III was the highest and most stabilized among three types.

The total precipitation of Type I, II, and III for two years was 30, 36, and 120mm, respectively. The first rain in 1993 was very strong and there were large deviations of the precipitations of each collector. Type III has collected 3 to 4 times as much precipitation amount as the others. This collection efficiency is in the same range as the value predicted in section 1.3.2 and the compensation coefficient of Table 1.1.

Table 1.2 Type III collection ratio of the average value in the port side to the average value of both sides.

Ion species	Average	Standard deviation
H ⁺	0.96	0.29
Cl ⁻	1.01	0.23
NO ₃ ⁻	1.05	0.25
SO ₄ ²⁻	1.00	0.22
Na ⁺	1.01	0.23
NH ₄ ⁺	1.02	0.25
K ⁺	1.01	0.22
Mg ²⁺	1.00	0.23
Ca ²⁺	1.01	0.24
nss-SO ₄ ²⁻	1.03	0.32
nss-Ca ²⁺	1.11	0.40
Precipitation amountt	0.96	0.17

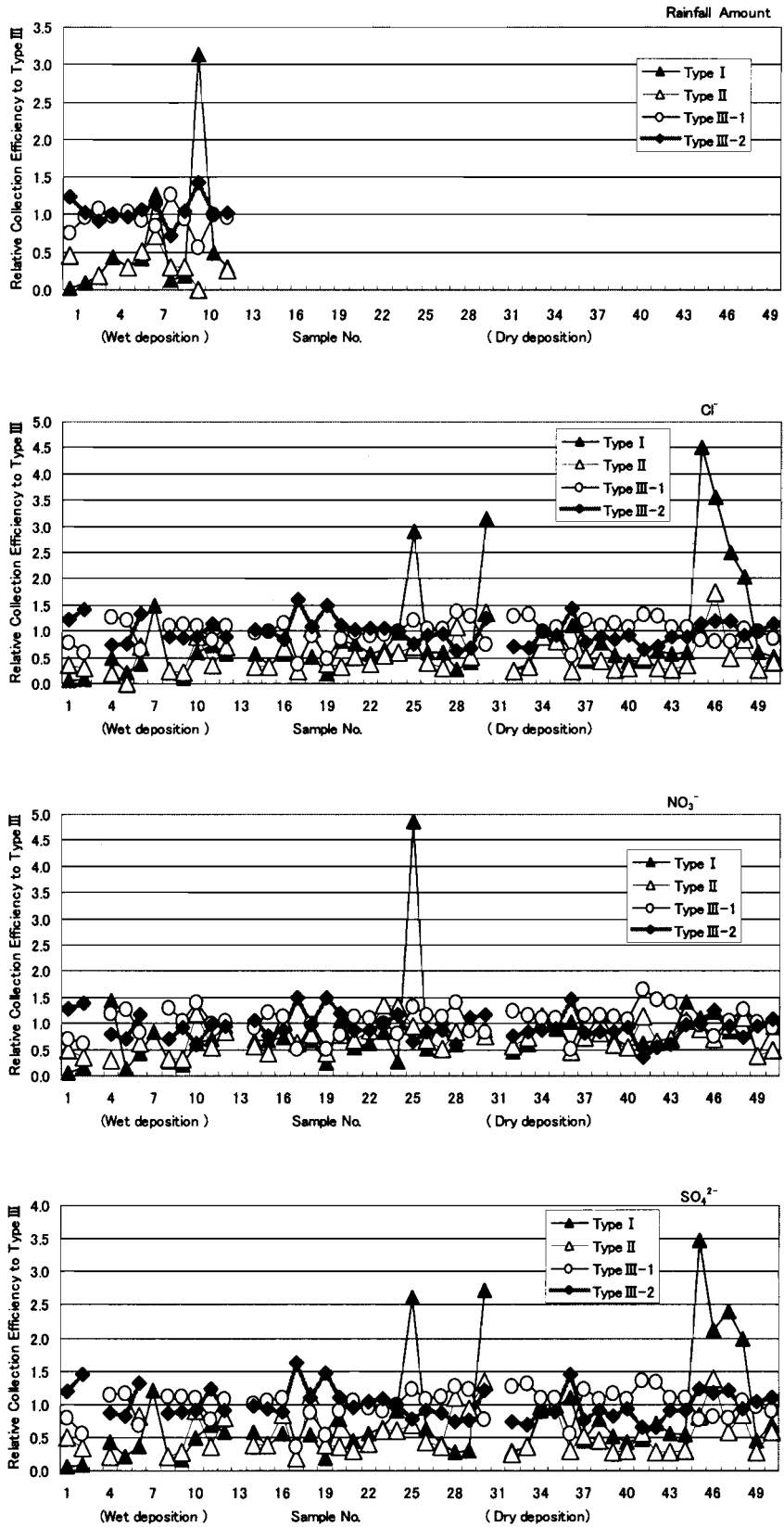


Figure 1.5 Relative collection efficiency .

1.3.4 Comparison of Collection Efficiency

The collection efficiency of each precipitation collector was evaluated on the basis of the average value of Type III that had the highest collection efficiency. The collection efficiency of each precipitation collector to the average of Type III is shown in Figure 1.5. 12 data on the left-hand side in the figure are wet deposition data, and 36 data on the right-hand side are dry deposition data. There are not so large difference between the collection efficiencies of ion species of wet and dry depositions. But Type III collected a larger amount of ionic species than Type I and II. Many of sea-salt components such as Cl^- and SO_4^{2-} were sampled twice as much ion species as the other equipments. As to NO_3^- , the difference of the collection efficiency between these equipments was small.

In addition, Type I sometimes shows unusually the high collection efficiency as for the precipitation amount, the collection efficiencies of the sample of Nos. 7 and 10 showed 100% or more. As for the ion species of wet deposition, the collection efficiency of No. 7 was high. As for the ion species of the dry deposition, those of Nos.25, 30, 36, 45, 46,47 and 48 were high. Wind speed was low when collected these samples.

Figure1.6 shows the median of the relative collection efficiency of each collector to the average of Type III. There is a clear tendency in the collection efficiency of an ion species, and the tendency was investigated based on this median of the relative collection efficiency to the average value of type III. As shown in Figure 1.6, except for H^+ , the collection efficiencies of Type I and II were lower compared with that of Type III. In these measurement items, the collection efficiency of rainfall amount was about 30%. In the ion species, as for NH_4^+ and nss- SO_4^{2-} (nss:non-sea-salt), the collection

efficiency of Type II showed higher than Type I. Moreover, as for ion species other than NH_4^+ and nss-SO_4^{2-} , Type I had higher collection efficiency than Type II. In addition, it seemed that NO_3^- had few differences between them.

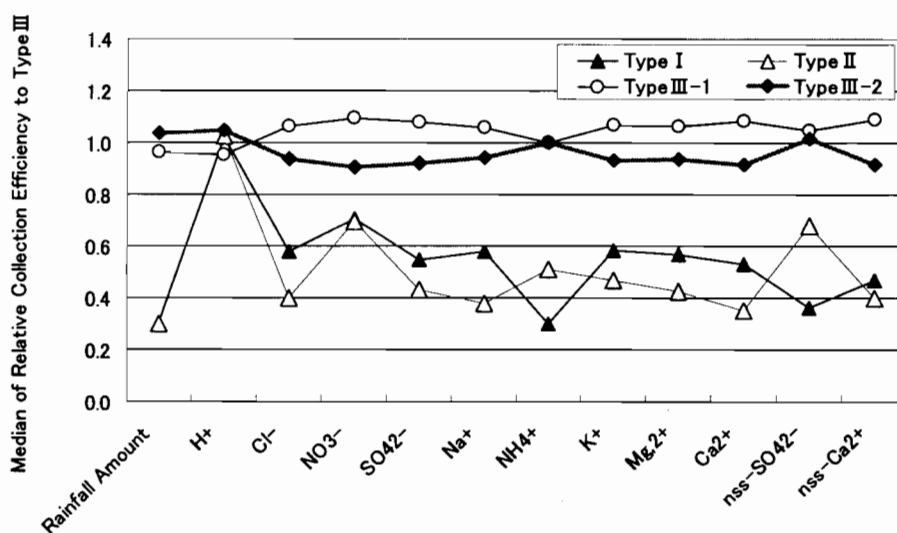


Figure1.6 Median of relative collection efficiency to Type III

Type I and Type III- 1 were installed in the port side of the deck.

Type II and Type III-2 were installed in the starboard of the deck.

1.4 Conclusion

Samplers for rainfall, throughfall, and stemflow were studied to develop a suitable simplified collection method for long-term monitoring of the effect of acid deposition on a forest ecosystem. A filtrating bulk sampler was modified for rainfall and throughfall samplings. The pH value and the main chemical components did not change in a two-week sampling period, and the sampler had high collection efficiency.

The Investigation on the collection method of rain and atmospheric depositions on board was conducted using three kinds of precipitation collectors. The precipitation collector of Type III which has a slant opening of the upper funnel could collect rain and ion species most effectively.

In the precipitation, Type III sampled 3 to 4 times as much as the others. The precipitation collector of Type III collected the ion species about twice as much as the others. The equipment of Type III will be suitable for the rain measurement on board under high wind conditions. Moreover, when more precise measurements of the precipitation and atmospheric depositions are needed, theoretical correction coefficient can apply to eliminate influence of wind.

References

- (1) Tamaki, M, 1997, List on Acid Rain Research in Japan, Research Institute of Environmental Technology (In Japanese).
- (2) Tamaki, M. and Hiraki, T., 1992, *Nihon Kagaku Kaishi*, 1992, 405 (In Japanese with English summary).
- (3) Hall, D.J. and S.L. Upton, 1988: A Wind Tunnel Study of the Particle Collection Efficiency of an Inverted Frisbee used as a Dust Deposition Gauge, *Atmospheric Environment*, 22, No. 7, 1383-1394.
- (4) Rasmussen, R., M. Dixon, F. Hage, J. Cole, C. Wade, J. Tuttle, S. McGettigan, L. Stevenson, W. Fellner, S. Knight, E. Karplus and N. Rehak, 2001: Weather Support to Deicing Decision Making (WSDDM): A Winter Weather Nowcasting System, *Bull. Amer. Meteorol. Soc.*, 82(4), 579-596.
- (5) Rasmussen, R. M., J. Hallett, R. Purcell, J. Cole¹, and M. Tryhane, 2002: The hotplate snowgauge, 10th Conference on Aviation, Range and Aerospace Meteorology, 13-16, May 2002, Portland OR.
- (6) Japan Environment Agency, 1999, Report on Phase-III Study of Acid Deposition Survey over Japan (In Japanese).

Chapter 2

Measurement of Atmospheric Deposition over the Western Pacific Equatorial Ocean

2.1 Introduction

During the last century, the composition of the atmospheric deposition has changed dramatically as a consequence of an increase in anthropogenic emissions, especially sulfur dioxide and nitrogen oxides. Consequently, the pH of rainwater is as low as four in various regions of the world (Galloway *et al.*⁽¹⁾). This decrease in the pH is often associated with an increase in sulfate ion (SO_4^{2-}) and nitrate ion (NO_3^-). The atmospheric deposition over the ocean is one of the major sink pathways of anthropogenic air pollutants (Galloway *et al.*⁽²⁾). In marine areas, sea-salt constituents characterize the atmospheric deposition. Although SO_4^{2-} is well known as an anthropogenic pollutant, it is also a sea-salt constituent. It is important to distinguish anthropogenic SO_4^{2-} (non-sea-salt SO_4^{2-} , hereafter referred to nss- SO_4^{2-}) from natural SO_4^{2-} .

The chemical composition of seawater shows the same composition ratio in various ocean. The coefficients of variation of $\text{SO}_4^{2-}/\text{Cl}^-$, Na^+/Cl^- , and $\text{Mg}^{2+}/\text{Cl}^-$ ratios in

various oceans are less than 1 % (Horne⁽³⁾). But the chemical composition of sea-salt particles generated by bubbles breaking on the surface is different from that of bulk seawater. Many of the anomalous ion ratios of marine constituents of atmospheric aerosols and rainwater are the result of an ion enrichment in aerosols dispersed from bursting bubbles (Hiraki *et al.*;⁽⁴⁾ Sugawara and Kawasaki⁽⁵⁾).

Garland⁽⁶⁾ showed that the ion fractionation of sea-salt particles might occur during the particle formation at the sea surface and the ratio of SO_4^{2-} to Na^+ in the spray exceeded the ratio of seawater by 10 to 30 %. Other processes of the modification of sea salt were found in polar snow (Gjessing;⁽⁷⁾ Hall and Wolff⁽⁸⁾) and in the coastal atmosphere (Okada *et al.*;⁽⁹⁾ Posfai *et al.*⁽¹⁰⁾). However, in this observational area, we do not believe that these modification processes occur.

In this research, the ion constituents of the atmospheric deposition in the equatorial sea area was measured on board the R/V MIRAI from June 9 through July 6, 1999, during the NAURU99 Experiment. The details of this experiment are described by Yoneyama.⁽¹¹⁾

2.2 Observation and Analytical Method

The atmospheric deposition observation was conducted during a cruise on board the R/V MIRAI from June 9 through July 6, 1999(Figure 2.1). The vessel sailed south from Yokohama, Japan, to the equatorial ocean at a speed of about 20 knots and with a constant heading from June 7 to June 18. For most parts, the vessel stayed at the observational station near Nauru Island from June 19 to July 6.

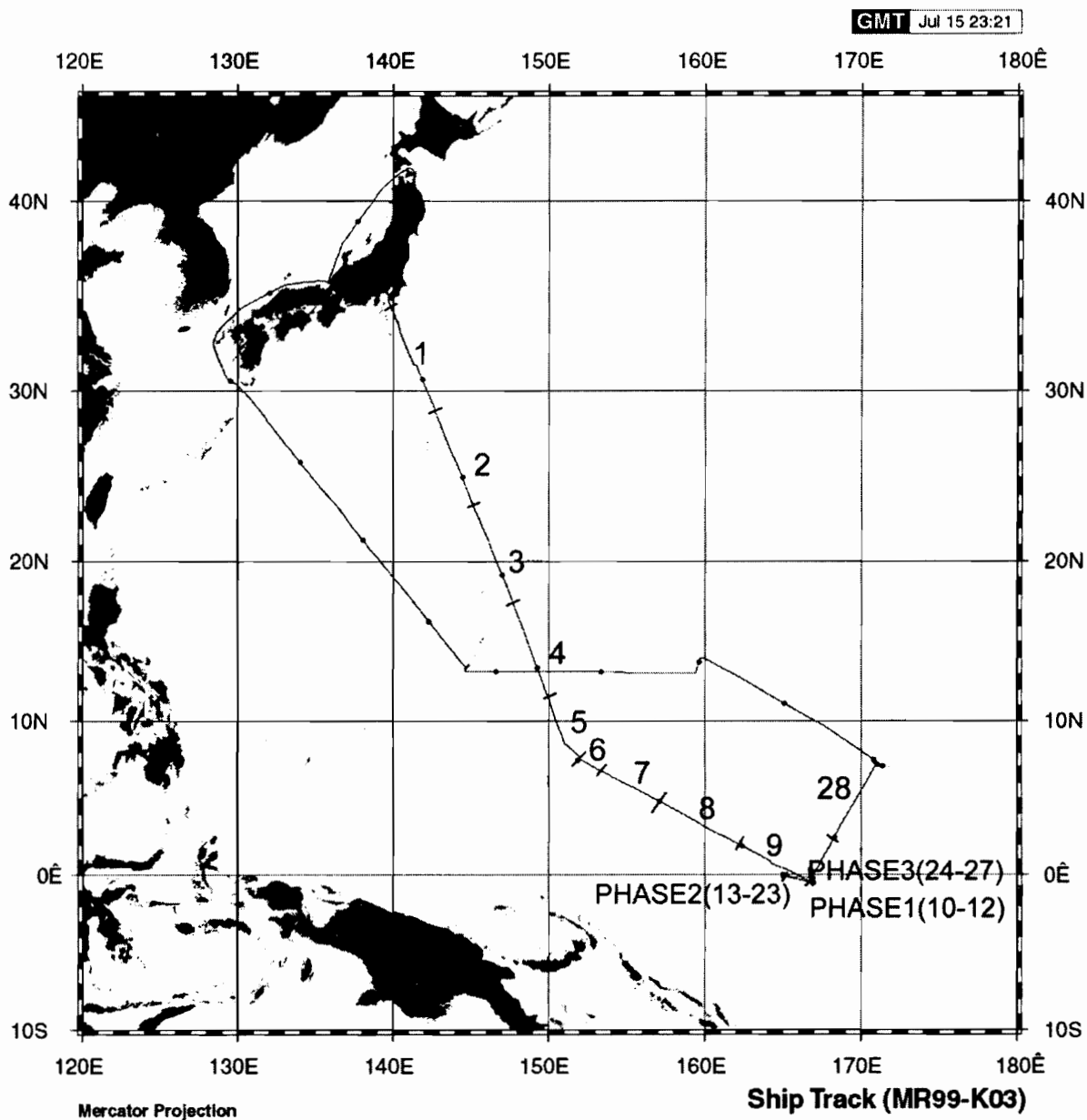


Figure 2.1 Ship track and sampling area number.

The atmospheric deposition sampler and its attachment gear are shown in Figure 2.2. The sampler consists of an upper funnel with a slant opening of 45 degrees and a lower reserve bottle. It is made from a 5-liter polyethylene bottle and is 650 mm high and 170 mm in diameter. The sampler has a filter that is 47 mm in diameter with a pore

size of $0.8 \mu\text{m}$ (Milipore, AAWP047) between two parts. This sampler was detailed in chapter 1. Two samplers were installed in the port and starboard sides on the roof of the anti-rolling tank approximately 20 m above the sea surface. The atmospheric deposition was sampled regularly at 11:00 ship's time (ship's time = UTC + 9 to 11 hours) everyday.

The atmospheric deposition sample has two classifications: during rain and no rain. When it was raining at the collection the samples, the sampled rainwater is referred to a wet deposition. When it was not raining, the upper funnel of the sampler was washed with 100 ml of distilled water, and the dissolved constituents are referred to dry deposition constituents.

Eight major ions (Na^+ , K^+ , NH_4^+ , Mg^{2+} , Ca^{2+} , SO_4^{2-} , NO_3^- , and Cl^-) of the atmospheric deposition were analyzed with a dual column system ion chromatograph (Dionex, DX300) equipped with an automatic sample injector. The analyses of electric conductivity and pH were carried out with a pH & EC meter (TOA, WM-50EG) equipped with an automatic sample changer and a water bath with 25°C .

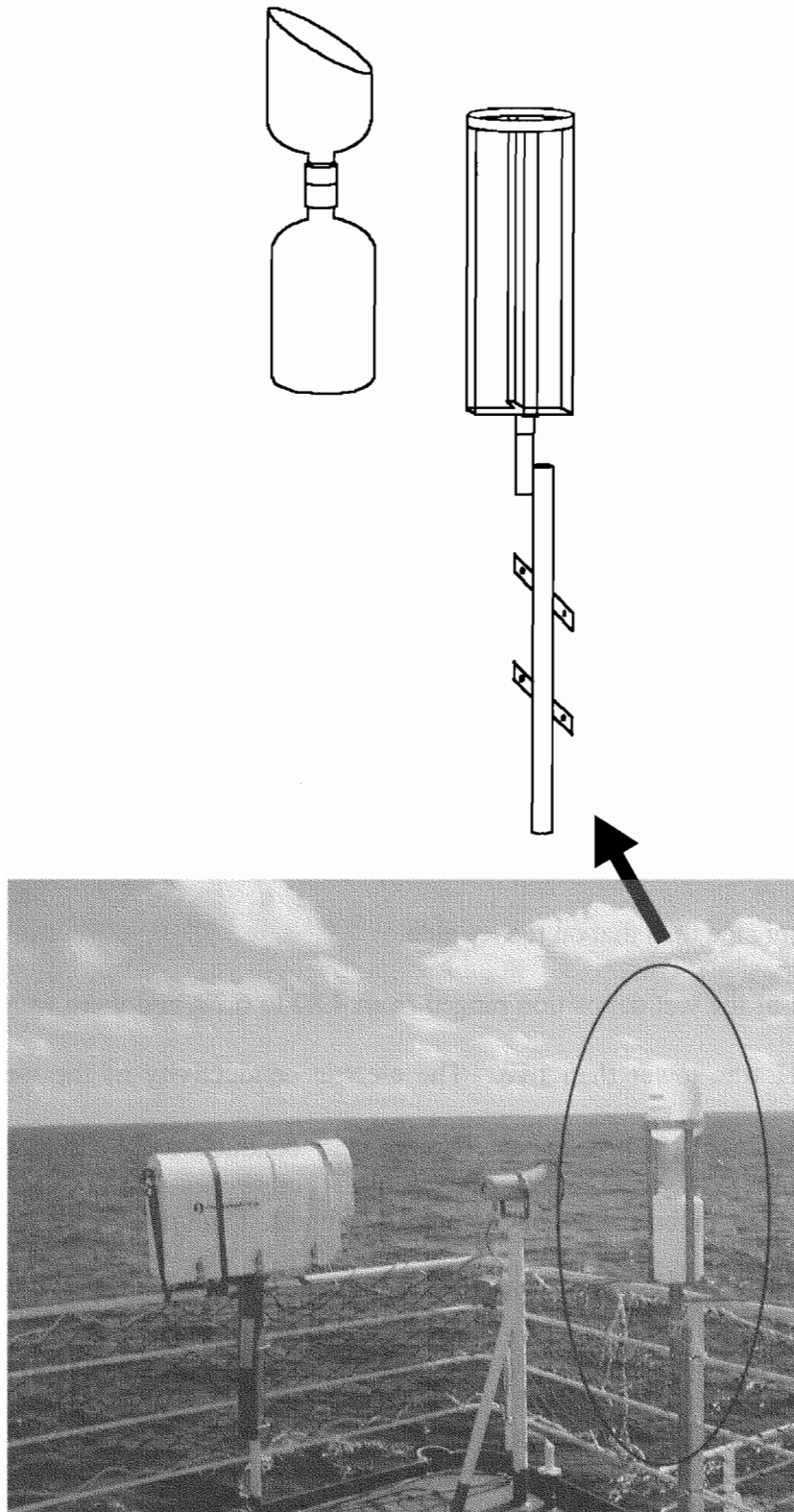


Figure 2.2 An atmospheric deposition sampler.

2.3 Results and discussion

2.3.1 Overview of the Atmospheric Deposition

It rained 16 times from June 9 to July 6, 1999, and 53 samples (27 wet and 26 dry depositions) were obtained (Table 2.1). Of the 27 wet depositions, samples were obtained from the port and starboard sides in 11 cases (22 samples) and from one side only in five cases (five samples). As listed in Table 2.2, total rainfall was about 261 and 308 mm, and the daily mean rainfall was 16.3 and 19.2 mm/day on the port and starboard sides, respectively. The maximum daily rainfall was 120 mm/day. The difference between rainfall on both sides was influenced by the relative wind direction. When wind blew from one side (port or starboard), the rainfall on that side tended to be heavier than that on the opposite side. In other words, the rainfall tended to be heavier on the weather side than that on the lee side.

The pH of the wet deposition ranged from 4.80 to 6.20, and there were three cases when the pH was lower than five. The electric conductivity of the wet deposition ranged from 2 to 2080 $\mu\text{S}/\text{cm}$. The electric conductivity of distilled water in equilibrium with carbon dioxide in the air is about 1 $\mu\text{S}/\text{cm}$. The lowest electric conductivity was 2 $\mu\text{S}/\text{cm}$. It was very close to the conductivity of distilled water.

The accuracy of the ion analysis is confirmed by a comparison of measured and calculated electric conductivities, as shown in Figure 2.3. Calculated electric conductivity is obtained from an equivalent concentration and equivalent conductance (Barrow⁽¹²⁾). The calculated electric conductivities are in quite good agreement with measured one. At the same time, the electric neutrality of ions, which is so-called ionic

budget, was also investigated to confirm the analytical accuracy. Figure 2.4 shows the ion budget of the atmospheric deposition and the relationship between the total cation and anion concentrations. The ionic budget was calculated from concentrations expressed in milli-equivalents per liter (meq.l^{-1}). The equilibrium in the ionic budget as well as the good agreement with the electric conductivity comparison suggest that no major ions have been missed in this analysis, demonstrating that the ion analysis was conducted with in high accuracy.

Table 2.1 Atmospheric deposition measurement in the Western Pacific
Equatorial Ocean

Date	Area No.	Position	Amount of rainfall (mm)	Sample Side	pH	E.C. (μS/cm)	Deposition (mmol/day/m ²)										
							Cl-	NO ₃ -	SO ₄ ²⁻	Na+	NH ₄ ⁺	K+	Mg ²⁺	Ca ²⁺	H+	Ainon	Cation
06/09/99	1	30N	71.4	Port	5.91	2080	1375	1.67	57.3	1168	0	21.6	122	24.8	0.088	1491	1483
06/10/99	2	25N	2.9	Port	5.65	1550	39.8	0.077	1.70	34.0	0	0.61	3.61	0.679	0.679	43.3	43.2
06/11/99	3	20N		Port	5.37	732	28.3	0.035	1.35	24.1	0	0.47	2.77	0.536	0.536	31.1	31.2
06/12/99	4	12N		Port	5.39	237	8.51	0.020	0.450	7.33	0	0.140	0.818	0.226	0.226	9.43	9.58
06/13/99	5	Chuuk	65.3	Port	5.31	35	17.0	0.053	0.892	15.0	0	0.256	1.54	0.430	0.430	18.9	19.6
06/14/99	6	Chuuk	0.0	Port	5.20	70	0.017	0	0.001	0.015	0	0.000	0.002	0.000	0.000	0.019	0.019
06/15/99	7	5N	8.7	Port	5.05	9	0.532	0.003	0.034	0.421	0	0.007	0.033	0.012	0.012	0.609	0.614
06/16/99	8	2N	90.2	Port	5.20	29	19.4	0.019	0.823	17.5	0	0.278	1.63	0.274	0.274	21.1	22.1
06/17/99	9	Phase 1	10.1	Port	5.09	27	1.93	0.005	0.099	1.73	0	0.030	0.169	0.030	0.030	2.14	2.24
06/18/99	10	Phase 1		Port													
06/19/99	11	Phase 1		Port	5.42	9	0.242	0.004	0.011	0.198	0.010	0.012	0.012	0.003	0.003	0.274	0.268
06/20/99	12	Phase 2	0.1	Port	5.70	57	0.026	0.001	0.001	0.022	0.005	0.001	0.003	0.001	0.001	0.031	0.035
06/21/99	13	Phase 2		Port	5.42	25	0.773	0.005	0.044	0.689	0	0.030	0.072	0.027	0.027	0.871	0.935
06/22/99	14	Phase 2		Port	5.02	10	0.203	0.003	0.014	0.152	0	0.008	0.009	0.004	0.004	0.235	0.229
06/23/99	15	Phase 2	0.0	Port	5.90	200	0.066	0	0.001	0.056	0	0.001	0.003	0.002	0.002	0.068	0.067
06/24/99	16	Phase 2		Port	5.50	16	0.358	0.003	0.009	0.303	0.015	0.022	0.012	0.010	0.010	0.385	0.398
06/25/99	17	Phase 2	1.6	Port	5.50	15	0.124	0.003	0.008	0.107	0.012	0.013	0.005	0.004	0.004	0.145	0.156
06/26/99	18	Phase 2		Port	5.18	5	0.122	0.002	0.006	0.064	0	0.003	0.003	0.004	0.004	0.139	0.109
06/27/99	19	Phase 2	1.0	Port	5.40	2	0.019	0	0.000	0.005	0	0.003	0	0.000	0.000	0.021	0.013
06/28/99	20	Phase 2	7.9	Port	4.83	24	1.03	0.009	0.066	0.914	0	0.019	0.083	0.032	0.032	1.17	1.28
06/29/99	21	Phase 2		Port	5.20	35	1.09	0.004	0.051	0.955	0	0.021	0.089	0.020	0.020	1.20	1.22
06/30/99	22	Phase 2		Port	5.10	10	0.254	0.003	0.014	0.202	0.004	0.008	0.013	0.005	0.005	0.287	0.285
07/01/99	23	Phase 3		Port	5.19	19	0.549	0.003	0.030	0.489	0	0.011	0.038	0.013	0.013	0.616	0.63
07/02/99	24	Phase 3	0.4	Port	5.20	12	0.024	0.000	0.000	0.020	0.003	0.001	0.001	0.000	0.000	0.026	0.028
07/03/99	25	Phase 3		Port	5.13	22	0.628	0.006	0.034	0.562	0.006	0.014	0.046	0.013	0.013	0.705	0.734
07/04/99	26	Phase 3		Port	4.73	19	0.392	0.002	0.018	0.348	0.004	0.013	0.020	0.006	0.006	0.431	0.498
07/05/99	27	2N		Port	5.07	136	4.74	0.006	0.158	4.15	0	0.095	0.382	0.091	0.091	5.06	5.23
07/06/99	28	Majuro	1.5	Port	4.90	149	1.23	0.005	0.069	1.05	0	0.025	0.114	0.037	0.037	1.38	1.40
06/09/99	1	30N	85.0	Star	5.87	1000	727	3.46	31.2	618	0	11.67	66.5	13.22	13.2	793	789
06/10/99	2	25N	2.9	Star	5.34	422	10.3	0.035	0.437	8.67	0	0.170	0.902	0.176	0.176	11.2	11.0
06/11/99	3	20N		Star	5.38	227	8.35	0.037	0.361	7.185	0	0.138	0.775	0.167	0.167	9.11	9.22
06/12/99	4	12N		Star	5.32	473	18.2	0.016	0.694	15.4	0	0.285	1.687	0.242	0.242	19.6	19.6
06/13/99	5	Chuuk	65.6	Star	5.20	25	12.2	0.033	0.630	10.7	0	0.170	1.017	0.247	0.247	13.6	13.9
06/14/99	6	Chuuk	0.6	Star	6.10	480	1.91	0.004	0.088	1.61	0	0.044	0.177	0.041	0.041	2.09	2.09
06/15/99	7	5N	8.4	Star	5.09	23	1.54	0.012	0.083	1.38	0.020	0.062	0.121	0.036	0.036	1.73	1.86
06/16/99	8	2N	120.9	Star	5.04	30	24.3	0	1.071	21.7	0	0.344	1.952	0.332	0.332	26.5	27.7
06/17/99	9	Phase 1	7.0	Star	5.18	75	4.37	0.009	0.194	3.72	0	0.070	0.394	0.072	0.072	4.77	4.77
06/18/99	10	Phase 1	0.3	Star	6.10	380	0.896	0.001	0.039	0.735	0.005	0.034	0.079	0.019	0.019	0.978	0.971
06/19/99	11	Phase 1		Star	4.82	16	0.332	0.004	0.021	0.279	0	0.009	0.028	0.009	0.009	0.380	0.428
06/20/99	12	Phase 2		Star													
06/21/99	13	Phase 2		Star	5.28	5	0.119	0	0.006	0.065	0	0.002	0.005	0.003	0.003	0.135	0.106
06/22/99	14	Phase 2		Star	5.30	4	0.113	0.002	0.004	0.057	0	0.003	0.003	0.002	0.002	0.128	0.091
06/23/99	15	Phase 2		Star													
06/24/99	16	Phase 2	0.0	Star	4.80	42	0.011	0	0.000	0.010	0	0.000	0.000	0.000	0.000	0.012	0.012
06/25/99	17	Phase 2	1.6	Star	6.20	86	0.577	0.008	0.013	0.550	0.146	0.141	0.019	0.024	0.024	0.625	0.925
06/26/99	18	Phase 2		Star	5.27	6	0.139	0.004	0.005	0.093	0	0.010	0.003	0.003	0.003	0.156	0.139
06/27/99	19	Phase 2	3.3	Star	5.31	3	0.059	0	0	0.011	0	0.010	0	0	0	0.062	0.038
06/28/99	20	Phase 2	9.3	Star	5.15	48	3.51	0.012	0.149	3.01	0	0.060	0.288	0.062	0.062	3.83	3.83
06/29/99	21	Phase 2		Star	5.16	32	1.04	0.004	0.047	0.914	0	0.018	0.087	0.017	0.017	1.14	1.17
06/30/99	22	Phase 2		Star	5.10	14	0.342	0.003	0.015	0.291	0	0.010	0.018	0.006	0.006	0.377	0.385
07/01/99	23	Phase 3		Star	5.10	20	0.456	0.003	0.019	0.402	0	0.007	0.029	0.007	0.007	0.499	0.517
07/02/99	24	Phase 3		Star	5.31	14	0.388	0.004	0.015	0.334	0.004	0.007	0.023	0.007	0.007	0.427	0.427
07/03/99	25	Phase 3		Star	5.08	18	0.510	0.004	0.023	0.458	0	0.013	0.035	0.009	0.009	0.562	0.596
07/04/99	26	Phase 3		Star	5.21	15	0.424	0.003	0.020	0.371	0	0.011	0.027	0.006	0.006	0.470	0.474
07/05/99	27	2N		Star	5.06	41	1.34	0.006	0.058	1.183	0	0.026	0.111	0.020	0.020	1.47	1.51
07/06/99	28	Majuro	3.1	Star	5.01	51	1.18	0.006	0.055	1.013	0	0.018	0.109	0.026	0.026	1.30	1.33

Each sampler was collected at 11:00 ship time everyday basically. 0: not detectable.

Table 2.2 Wind direction dependence of precipitation anomaly on shipboard.

Wind direction	Port side rainfall amount (mm)	Starboard rainfall amount (mm)
Port	84.5	81.6
Starboard	176.6	226.1
Total(average)	261.1(16.3)	307.7(19.2)

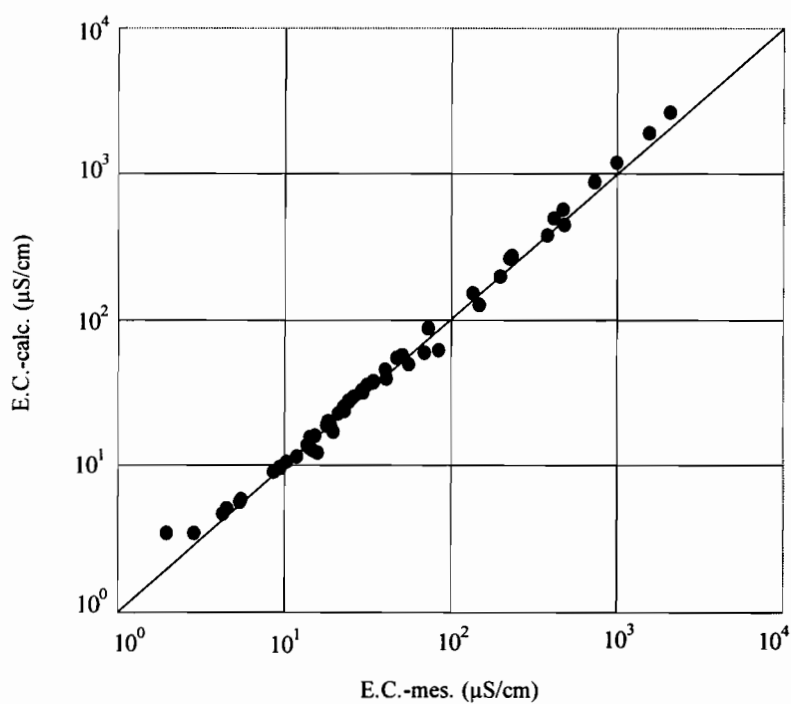


Figure 2.3 A comparison of the calculated with the measured electric conductivity.

E.C.-mes. and E.C.-calc. are the measured and the calculated electric conductivities, respectively.

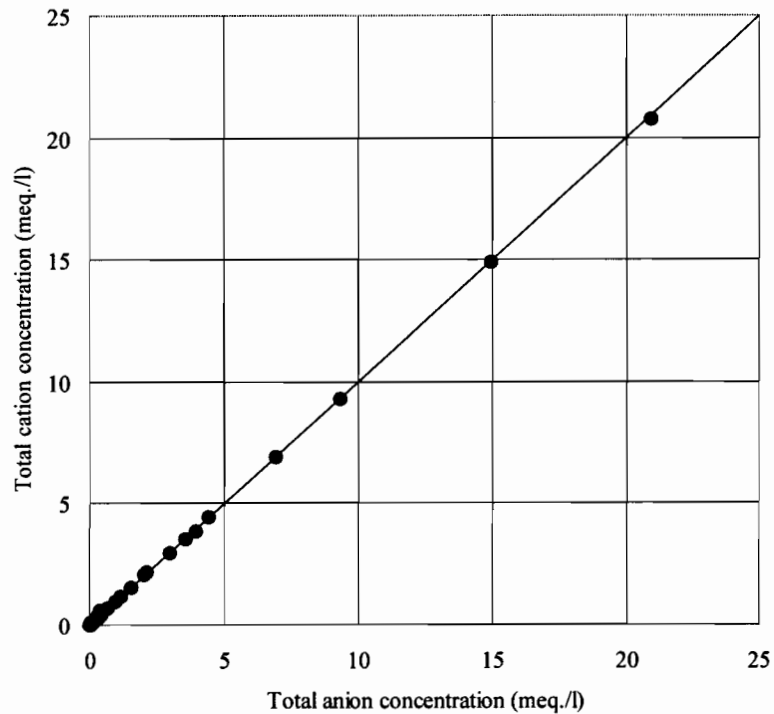


Figure 2.4 The ionic budget of an atmospheric deposition.

2.3.2 Wet and Dry Depositions

A dry deposition depends on aerosol concentration, size, and hygroscopicity, assuming that atmospheric and oceanic conditions are ordinary. Parungo *et al.*⁽¹³⁾ measured wet and dry depositions over the Pacific Ocean, and they concluded that, for small nss-SO_4^{2-} or NH_4^+ , a wet deposition is more important for removing aerosols from the atmosphere than a dry deposition. For sea-salt and terrestrial particles, wet and dry depositions are almost equal to each other in the Western Pacific Equatorial Ocean.

The time series of the Na^+ deposition is shown in Figure 2.5. The Na^+ deposition tended to decrease as the vessel sailed south, except for an unusual deposition caused by a storm at the beginning of the voyage, and tended to be relatively constant when the vessel stayed on the equatorial ocean. The variation in the Na^+ deposition of the dry deposition is smaller than the Na^+ deposition of the wet deposition, and the dry Na^+ deposition is within the variation range of the wet Na^+ one. Therefore, it is concluded that both wet and dry depositions are about equal to each other in order of magnitude in this area although the wet deposition varies largely.

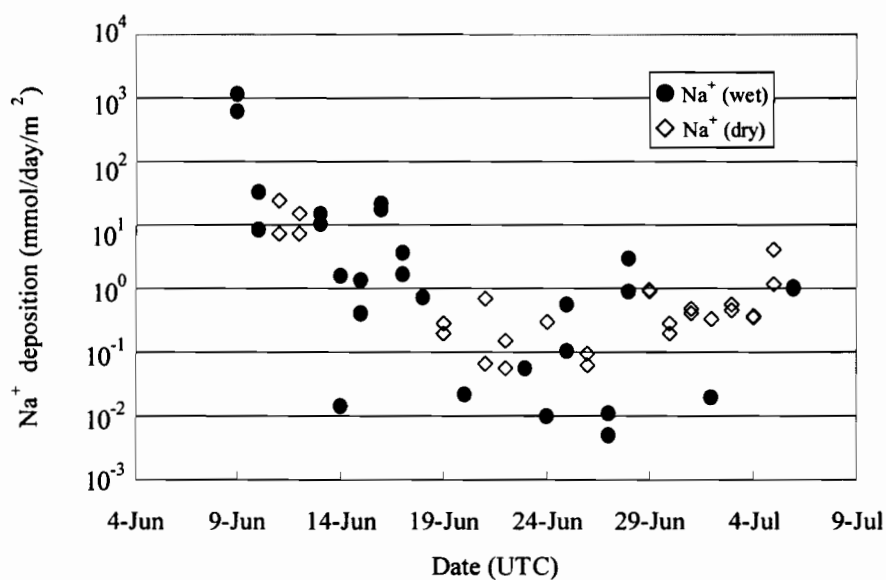


Figure 2.5 The time series of a Na^+ deposition.

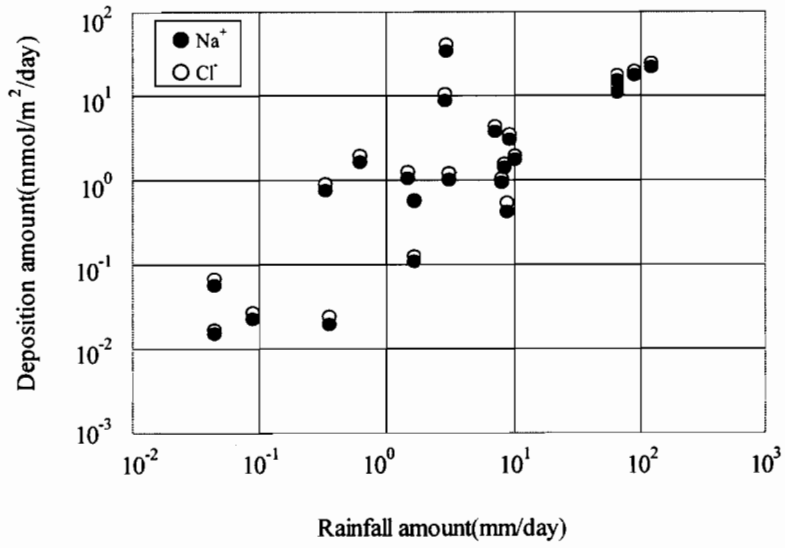


Figure 2.6 The relationship between deposition amount and rainfall amount.

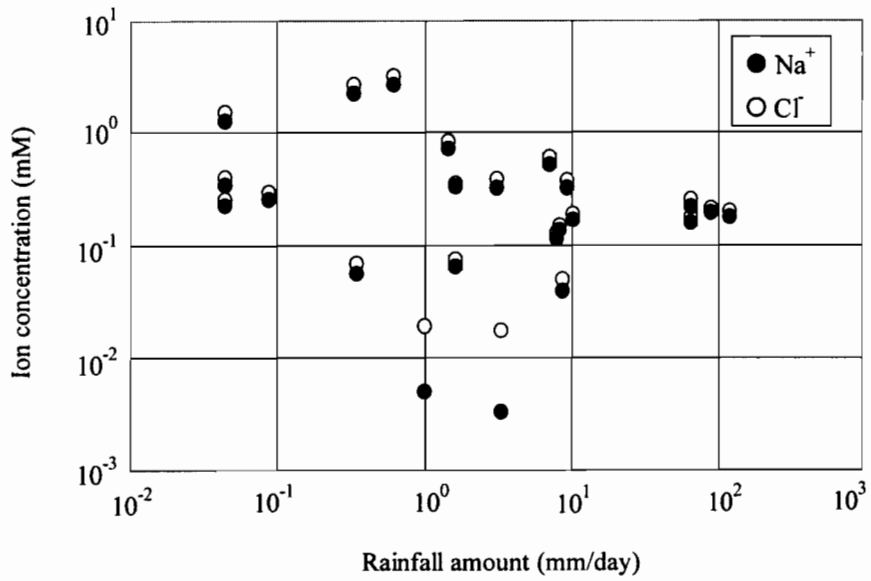


Figure 2.7 The relationship between ion concentration and rainfall.

Figure 2.6 shows the relationship between the depositions of Na^+ as well as Cl^- and the rainfall. Two pieces of data were omitted here because of the big differences in the depositions of Na^+ and Cl^- . Although the variation in the depositions is quite large, it tends to increase when the rainfall increases. These results are equivalent to those of Barrie.⁽¹⁴⁾

Figure 2.7 shows the relationship between the concentrations of Na^+ as well as Cl^- and the amount of rainfall. The data used here is the same as Figure 2.6. The ion concentration is nearly constant although it tends to decrease slightly, and most of the concentrations range from 0.1 to 1.0 mM. The concentrations of sea-salt constituents in the atmosphere do not decrease even when the rainfall increases. This disagrees with the results of Barrie.⁽¹⁴⁾

Therefore, it is concluded that sea-salt constituents were supplied simultaneously with water vapor from the sea surface in this area of the sea and the ratio of the generation rate of sea-salt particles to the evaporation rate is relatively constant.

2.3.3 Chemical Constituent of Atmospheric Deposition

Some investigators evaluated SO_4^{2-} of the marine origin in the total SO_4^{2-} of the atmospheric deposition and found that the ratio of SO_4^{2-} to Na^+ and a major component of seawater are the same in sea-salt aerosols and in bulk seawater (e.g., Hiraki *et al.*;⁽³⁾ Parungo *et al.*⁽¹³⁾). Non-sea-salt SO_4^{2-} was called nss- SO_4^{2-} which was calculated as follow: $[\text{nss-SO}_4^{2-}] = [\text{SO}_4^{2-}] - 0.0607[\text{Na}^+]$ mol/l. Most of the previously observed data showed a small amount of nss- SO_4^{2-} .

In the coastal area facing the Japan Sea, a large deposition of nss- SO_4^{2-} was reported by Hiraki *et al.*⁽³⁾ Since the increase in the deposition of nss- SO_4^{2-} was

consistent with the increase of the deposition of sea-salt compositions, the mole ratio of the major constituents of seawater to the Na^+ increased. The modification of seawater should be taken into consideration. In the coastal area of the Antarctic Ocean, negative nss-SO_4^{2-} was reported in aerosols by Hall.⁽⁸⁾

In this area, the concentration of atmospheric contaminants was quite low, and the sum of Na^+ and Cl^- in the atmospheric deposition was about 82 % of the total deposition. Figure 2.8 shows the ratio of the total ion concentration of sea salt to the total ion concentration of the atmospheric deposition from June 9 to July 6. The variation in the ratio is relatively small, and the ratio ranges from 80 to 96 %. The average ratio is 90 %.

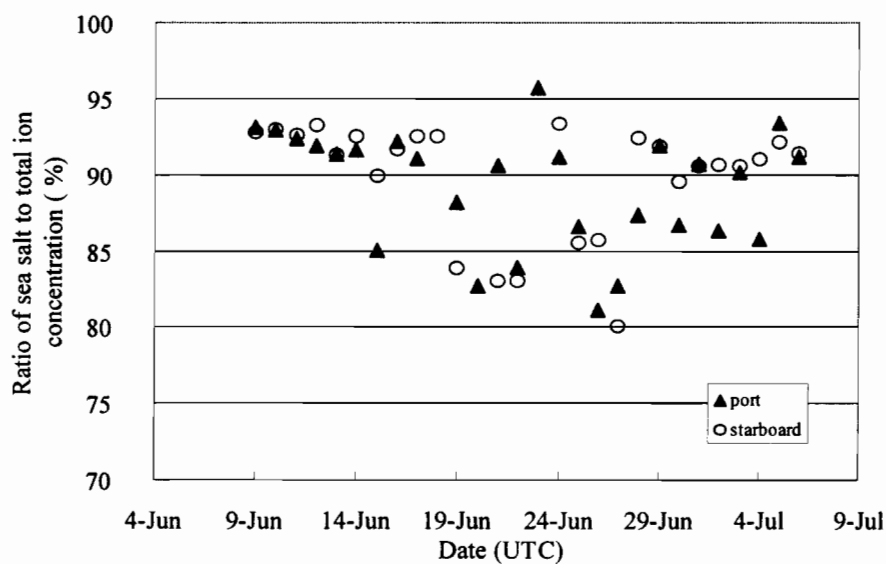


Figure 2.8 The ratio of sea salt to total ion concentration.

Table 2.3 Correlation coefficient matrixes among constituents of atmospheric

		Correlation coefficient of ion deposition amount								
		Cl ⁻	NO ₃ ⁻	SO ₄ ²⁻	Na ⁺	NH ₄ ⁺	K ⁺	Mg ²⁺	Ca ²⁺	H ⁺
Correlation coefficient of ion concentration	Cl ⁻		0.80	1.00	1.00	-0.05	1.00	1.00	1.00	0.04
	NO ₃ ⁻	0.81		0.80	0.80	-0.04	0.80	0.81	0.80	0.04
	SO ₄ ²⁻	1.00	0.82		1.00	-0.05	1.00	1.00	1.00	0.04
	Na ⁺	1.00	0.81	1.00		-0.05	1.00	1.00	1.00	0.04
	NH ₄ ⁺	-0.07	0.09	-0.07	-0.07		-0.04	-0.05	-0.05	-0.08
	K ⁺	0.97	0.80	0.97	0.97	0.11		1.00	1.00	0.04
	Mg ²⁺	1.00	0.82	1.00	1.00	-0.07	0.97		1.00	0.04
	Ca ²⁺	1.00	0.81	0.99	1.00	-0.05	0.97	0.99		0.04
	H ⁺	-0.38	-0.41	-0.38	-0.38	-0.30	-0.46	-0.38	-0.40	

Table 2.3 shows the correlation analyses of the deposition and the ion concentration of the major ions in the atmospheric deposition. The correlation coefficients of the deposition and the ion concentrations of Cl⁻, SO₄²⁻, Na⁺, K⁺, Mg²⁺, and Ca²⁺ were almost one. The coefficients of NO₃⁻ were about 0.8 except for NH₄⁺ and H⁺. The coefficients of NH₄⁺ and H⁺ were also quite low. Therefore, it is concluded that NH₄⁺ and H⁺ did not originate from sea salt but the other major ions did. However, there were some non-marine NO₃⁻, the NO₃⁻/Na⁺ mole ratio was very low at about 0.002.

The correlations between Na⁺ and other sea-salt constituents are extremely good, as seen in Figure 2.8. The molar ratios of the sea-salt constituents to Na⁺ are listed in

Table 2.4, in with those of standard seawater are also indicated. Since these mole ratios had good agreement with each other, no modification of sea-salt constituents occurred.

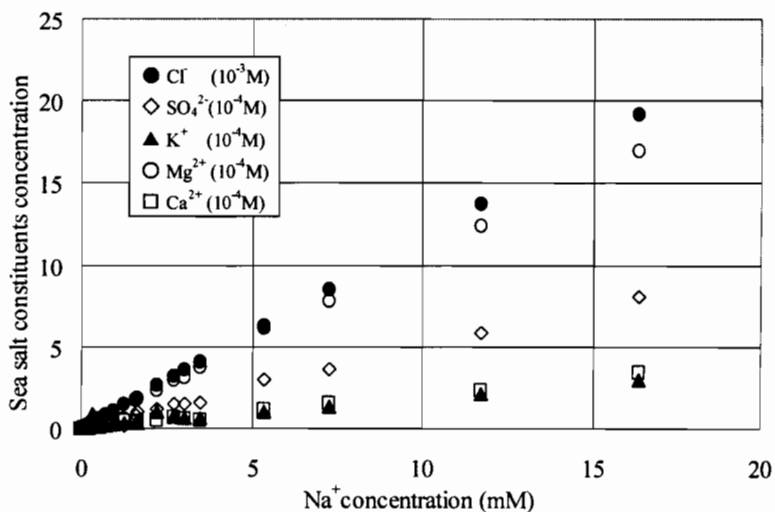


Figure 2.8 The relationship between sea-salt constituents and Na⁺ concentrations in an atmospheric deposition.

Table 2.4 Mole ratios of ion species in sea salt constituent to sodium ion

Ion	(mole ratio of ion/Na ⁺)	
	Standard seawater	This investigation
Cl ⁻	1.176	1.176
SO ₄ ²⁻	0.060	0.050
Mg ²⁺	0.115	0.106
Ca ²⁺	0.022	0.021
K ⁺	0.020	0.018

2.3.4 Acidity of Deposition

The pH value of distilled water was estimated to be 5.6 under the conditions of 25°C, 1 atm, and 350 ppm CO₂ in the air. Furthermore, the electric conductivity of this distilled water showed about 1 μ S/cm. However, the acidity of rainwater in a clean area was about pH=5 with the influence of natural SO₂. In this investigation, the pH values of both wet and dry depositions were from 4.73 to 6.20, and electric conductivity was from 2 to 2080 μ S/cm. Electric conductivity showed the minimum value at pH 5.4.

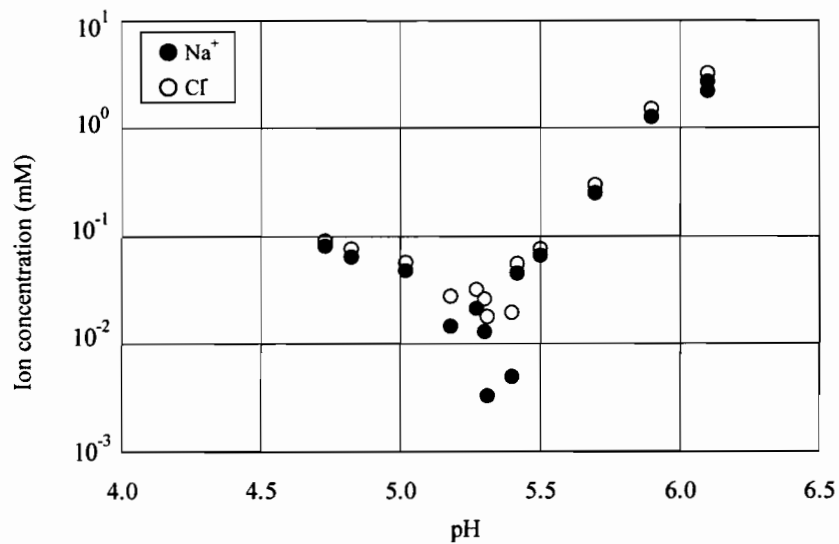


Figure 2.10 The relationship between ion concentration and pH.

In order to simplify the relationship between pH and the ion concentration of Na^+ and Cl^- which were the main constituents of the atmospheric deposition, the minimum concentrations were plotted in each pH, as shown in Figure 2.10. As seen in Figure 2.10, the concentrations increase in both cases when the atmospheric deposition is acidified from about pH 5.4 to pH 4.7 and neutralized from pH 5.4 to pH 6.1. It is reasonable that the deposition is neutralized by sea-salt alkalinity. However, the reason that the deposition is acidified is not clear.

Since the atmospheric deposition has the same constituent ratios as those of seawater, the acidity of the atmospheric deposition and seawater should be investigated. The relationship between the acidity of seawater and the HCO_3^- ion concentration is written in the following equation:

(1) $\text{CO}_2 + \text{H}_2\text{O} \rightarrow \text{H}_2\text{CO}_3$, Henry's law constant: 1.64×10^6 Pa at 25°C , CO_2 : 350 ppm in air.

(2) $\text{H}_2\text{CO}_3 \rightarrow \text{H}^+ + \text{HCO}_3^-$, $\text{pK} = 6.35$ at 25°C .

The HCO_3^- concentration of seawater is 2.35 mM, and ion activity is 0.504.

(3) $[\text{H}^+] = 10^{-6.35} \times [\text{H}_2\text{CO}_3] / [\text{HCO}_3^-]$,

(4) $[\text{H}^+] = 5.36 \times 10^{-12} / [\text{HCO}_3^-]$.

The initial ion concentrations of H^+ and HCO_3^- are $[\text{H}^+]_0$ and $[\text{HCO}_3^-]_0$, and the final ones are $[\text{H}^+]_f$ and $[\text{HCO}_3^-]_f$, as defined below. $[\text{H}^+]_f$ and $[\text{HCO}_3^-]_f$ are the concentrations when seawater is diluted with distilled water by the dilution factor D.

$[\text{H}^+]_0 = 2.28 \times 10^{-9} = X_0$, $[\text{HCO}_3^-]_0 = 2.35 \times 10^{-3} = Y_0$,

$[\text{H}^+]_f = X$, $[\text{HCO}_3^-]_f = Y$.

The following relations among these values are

(5) $X = X_0/D + C$, $Y = Y_0/D + C$,

where C is the increased concentration by absorption of CO₂ in air. From Equation (3), the ratio of [H⁺][HCO₃⁻]/[H₂CO₃] is constant even if seawater is diluted. [H₂CO₃] is constant under the same atmospheric condition. Therefore, it results in

$$(6) XY = X_0 Y_0 = 5.36 \times 10^{-12}.$$

These three formulas of (5) and (6) are solved and make the formulae of D and C.

$$C^2 + C(X_0 + Y_0)/D + 5.36 \times 10^{-12}(D^{-2} - 1) = 0,$$

$$C = \{-2.35 \times 10^{-3} D + [(2.35 \times 10^{-3})^2 - 2.144 \times 10^{-11}(D^{-2} - 1)]^{1/2}\} / 2.$$

The relationship between pH and the dilution factor estimated from the sea-salt concentration in the atmospheric deposition is shown in Figure 2.11, in which the pH of diluted seawater is shown by a solid line. The difference between the solid line and measured values results from the influence of non-sea-salt SO₄²⁻ and NO₃⁻.

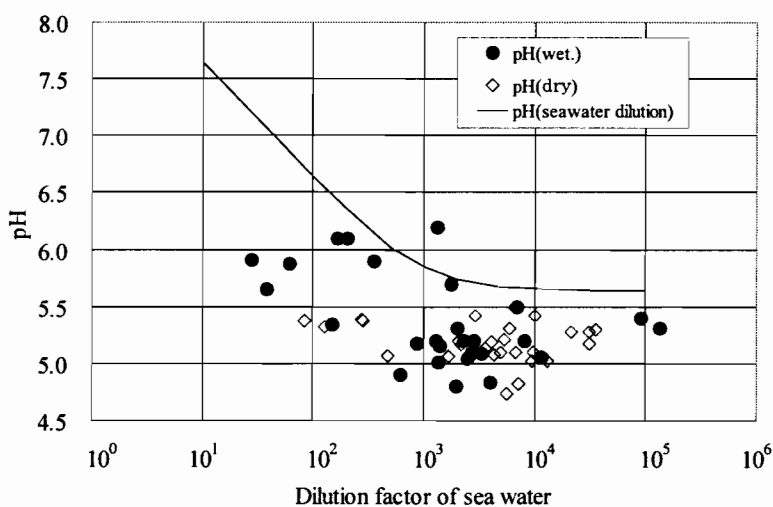


Figure 2.11 The relationship between pH and the dilution factor.

The solid line is a calculated pH value of diluted seawater.

3.3.5 Generation of Sea-Salt Particle

In marine areas, wave action entrains air and forms bubbles in the surface of sea water. The entrained bubbles then rise to the surface. The bubbles burst when they reach the surface and produce small droplets that are ejected into the air. Two types of drops have been distinguished, jet drops and film drops. Jet drops are produced from the jet of the water, which rises from the bottom of the collapsing bubble. Film drops are produced from the bursting of the water film forming the bubble. Particles with a wide range of sizes from about 0.1 to 100 μm are formed by these two production processes.

Woodcock⁽¹⁵⁾ measured a large difference in the number and size of sea-salt particles in marine air over the sea as a function of the altitude, position, and time. Then he found out that an increase in sea-salt particles near a cloud base was related to an increase in wind force. We obtained a similar result when the Na^+ deposition increased exponentially with increasing wind speed, as seen in Figure 2.12. Therefore, the atmospheric deposition increased with wind speed because the Na^+ deposition is the main constituent of the atmospheric deposition.

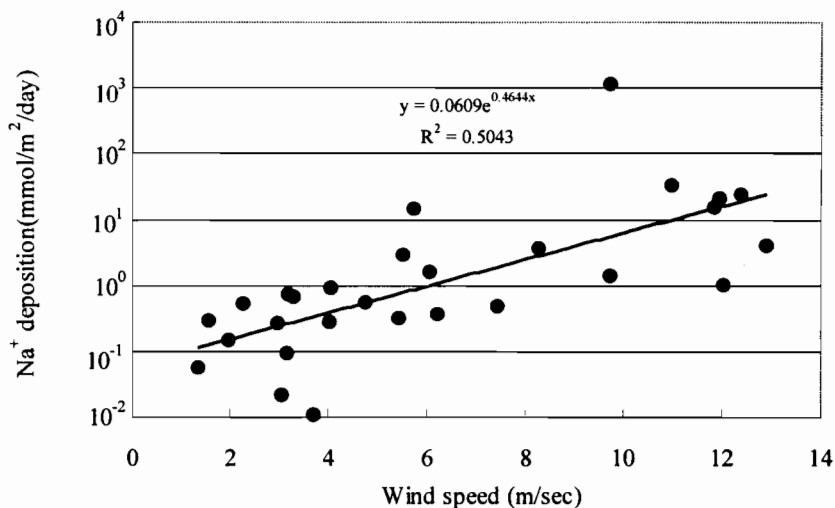


Figure 2.12 The relationship between the Na⁺ deposition and wind speed.

The solid line shows the regression line.

2.4 Conclusion

We analyzed 53 deposition samples for 28 days from June 9 to July 6, 1999. They were measured on board as the R/V MIRAI of JAMSTEC cruised during the NAURU99 Experiment on the Western Pacific Equatorial Ocean. It rained 16 times, and 27 wet deposition samples were obtained. The pH value of the wet depositions ranged from 4.80 to 6.20 and was lower than pH 5 in three samples. The electric conductivity of the wet depositions ranged from 2 to 2080 $\mu\text{S}/\text{cm}$.

Regarding both wet and dry sample depositions, the ionic budget of the atmospheric deposition was satisfactorily balanced when the concentrations of nine major ions (H^+ , Na^+ , K^+ , NH_4^+ , Mg^{2+} , Ca^{2+} , SO_4^{2-} , NO_3^- , and Cl^-) are taken into account. Na^+ , K^+ , Mg^{2+} , Ca^{2+} , SO_4^{2-} , and Cl^- are the typical constituents of sea-salt particles, which form one part of atmospheric aerosols over the ocean, and the molar ratio shows good agreement with the ratio of seawater. We could explain the acidity of the deposition by dilution of seawater. NO_3^- and NH_4^+ are linked to the difference between the predicted and observed values.

Winds cause a surge in the sea surface and generate sea-salt particles. A deposition increases exponentially as the wind speed increases.

References

- (1) Galloway, J. N., G. E. Likens, W. C. Keene, and J. M. Miller (1982): The composition of precipitation in remote areas of the world, *J. Geophys. Res.*, 87, 8771-8785.
- (2) Galloway, J. N., J. D. Thornton, S. A. Norton, H. L. Volchok, and R. A. MacLean (1982): Trace metals in atmospheric deposition: A review and assessment, *Atmospheric Environment*, 16, 1677-1700.
- (3) Horne, R. A. (1969): *Marine Chemistry*, Wilkey Interscience, New York.

- (4) Hiraki, T., M. Tamaki, and Y. Torihashi (1988): Influence of seasalt particle on atmospheric deposition, Report of the Environmental Science Institute of Hyogo prefecture, 20, 13-22 (in Japanese).
- (5) Sugawara, K., and N. Kawasaki (1958): Strontium and calcium distribution in the western Pacific, Indian, and Antarctic Oceans, Rec. Oceanogr. Works Japan, sp. No.2, 227-242.
- (6) Garland, J. A. (1981): Enrichment of sulphate in maritime aerosols, Atmospheric Environment, 15(5), 787 -791.
- (7) Gjessing, Y. (1989): Excess and deficit of sulfate in polar snow, Atmospheric Environment, 23(1), 155-160.
- (8) Hall, J. S., and E. W. Wolff (1998): Causes of seasonal and daily variations in aerosol sea-salt concentrations at a coastal Antarctic station, Atmospheric Environment, 32(21), 3669-3677.
- (9) Okada, K., Y. Ishizaka, T. Masuzawa, and K. Isono (1978): Chlorine deficiency in coastal aerosols, J. Meteorol. Soc. of Japan, 56, 501-507.
- (10) Posfai, M., J. R. Anderson, P. R. Buseck, T. W. Shattuck, and N. W. Tindale (1994): Constituents of a remote Pacific marine aerosol: A TEM study, Atmospheric Environment, 28(10), 1747-1756.
- (11) Yoneyama, K. (1999): Overview of (Note: It appears that something was omitted here. Please check and change as appropriate.)
- (12) Barrow, G. M. (1966): Physical Chemistry, McGraw-Hill, pp.677.

- (13) Parungo, F., C. Nagamoto, M. Y. Zhou, and N. Zhang (1992): Wet and dry deposition of atmospheric aerosols to the Pacific Ocean, The Fifth Intern. Conf. on Precipitation Scavenging and Atmosphere-Surface Exchange Processes, vol. 1, Precipitation Scavenging Processes, ISBN: 1560322632, 867-881.
- (14) Barrie, L. (1985): Scavenging ratio, wet deposition, and in-cloud oxidation; an application to the oxides of sulfur and nitrogen, *J. Geophys. Res.*, 90, 5789-5799.
- (15) Woodcock, A. H. (1953): Salt nuclei in marine air as a function of altitude and wind force, *J. Meteorol.*, 10, 362-371.

Chapter 3

Characteristics of Atmospheric Deposition over the North Pacific Ocean

3.1 Introduction

Atmospheric depositions contaminated by anthropogenic pollutants are spread worldwide, and this contamination is becoming an important international political issue. Atmospheric pollutants emitted from East Asia including Japan are transported far away and spread mainly over the North Pacific Ocean by westerly winds and then deposited. However, the deposition processes have not been clarified. Since so much sea-salt is deposited, it is usually quite difficult to estimate the amount of anthropogenic pollutants in the marine air. Hiraki *et al.*⁽¹⁾ proposed a method to evaluate the acidity of atmospheric depositions.

Based on on-board measurements taken in the North Pacific Ocean, Miyake *et al.*⁽²⁾ discovered that terrestrial aerosols diminished proportionally to the distance from the land and that there were some special locations where $[\text{SO}_4^{2-}]$ (hereafter [] denotes the concentration of an ion) was high in the Central North Pacific Ocean. They suggested the possibility that a highly contaminated air mass exists in some areas far from land in the Central North Pacific Ocean.

This investigation on atmospheric depositions was carried out on board of the T/S Nippon Maru, a tall sailing ship of the National Institute for Sea Training, Independent Administrative Institution of Japan, during a cruise in the North Pacific Ocean from June to August 1992. The ship emits only slight combustion exhaust and, therefore, does not contribute much contamination to the surrounding air. This paper describes the chemical characteristics of atmospheric depositions in the North Pacific Ocean based on on-board observations.

3.2 Observation and Analytical Method

The T/S Nippon Maru is a 2,570-ton four-masted bark with two supplemental diesel engines. The cruising route from June 22 through August 28, 1992, is shown in Figure 3.1. The dotted points and numerals in the figure are the data sampling positions and dates (day/month), respectively. She departed at Yokohama, Japan, on June 22 for Vancouver, Canada, and arrived there on July 20. She then departed at Vancouver for Honolulu, Hawaii, on July 27 and arrived there on August 7. After anchoring at Honolulu for a week, she departed for Tokyo on August 14. After departing at Honolulu, painting was taken place on deck; therefore, atmospheric deposition sampling was delayed for a week to avoid any possibility of chemical contamination. She arrived at Tokyo on August 28. On-board observations were made for 46 days during her 71-day cruise.

The atmospheric deposition sampler is made of polyethylene. It consists of an upper collection funnel and a lower reserve bottle, which were made from 5-liter

polyethylene bottles (the height and diameter are 650 and 170 mm, respectively) connected with a filter holder. This sampler was installed on the roof of the navigational bridge at a height of about 15 m above sea level. The details of the sampler are described by Hiraki *et al.*⁽³⁾.

Atmospheric depositions were routinely sampled once a day at noon of ship's time. When it rained for the sampling duration (about 24 hours), rainwater was reserved in a 100-ml polyethylene bottle. Sampled rainwater is regarded as wet deposition. When it did not rain, the upper collection funnel was washed out with 100 ml of distilled water, and the washed-out distilled water was collected and held in the bottle. This washed-out distilled water is the dry deposition. After the sample was collected, the upper collection funnel was washed with distilled water.

The observation was carried out for totally 46 days on board during the 71-day cruise. Therefore, the atmospheric deposition samples were obtained 46 times. Thirty-four collections were taken place during rainfall, and 12 in dry weather. The pH and electric conductivity of atmospheric depositions were measured on board with pH and electric conductivity meters (C-1 and C-127, Horiba, respectively), respectively, and the samples were stored in the refrigerator 4°C during the cruise. After completing the cruise, pH and electric conductivity were measured again with other instruments (501, Orion and CM-07, Kyoto Electric, Inc., respectively), and the major chemical constituents of atmospheric depositions (Na^+ , K^+ , Ca^{2+} , Mg^{2+} , NH_4^+ , Cl^- , SO_4^{2-} , and NO_3^-) were analyzed with ion chromatograph (DX300, Dionex) in the laboratory.

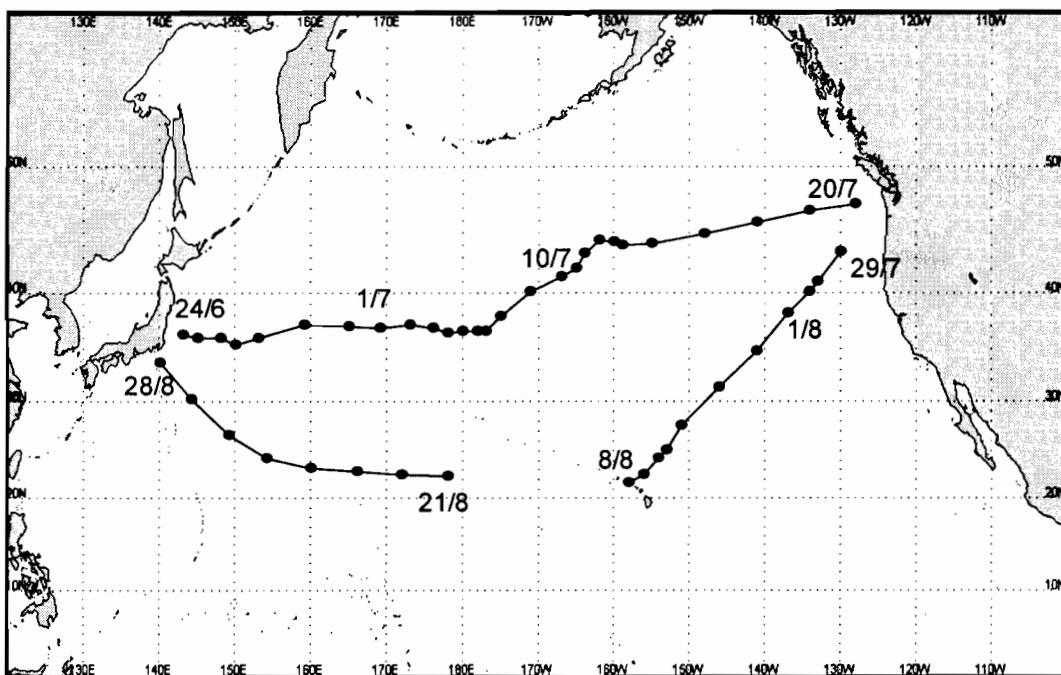


Figure 3.1 The cruising route of the T/S Nippon Maru. The dots and numerals show the sampling positions and dates (day/month), respectively.

3.3 Chemical Analyses

3.3.1 Evaluation of Analytical Quality

The pH value and electric conductivity of wet and dry atmospheric depositions measured on board and in the laboratory were in quite good agreement. Therefore, no quality changes in the samples occurred during the cruise. To examine the analytical accuracy of the atmospheric depositions, two tests were conducted according to the method proposed by The Research Group of Acid-rain Investigating Method ⁽⁴⁾. One test compares the electric conductivity of measured and theoretically calculated

estimates. The electric conductivity (EC) comparison was performed with the following calculations:

$R_{EC} = (\text{calculated EC}) / (\text{measured EC})$: R_{EC} was in the 0.96-1.32 range in this observation.

The other is the so-called ion budget test. The ion budget test examines the balance of anions to cations in a sample and confirms the balance in equivalent concentrations. The ion budget test was performed with the following calculations :

$R_{ION} = [\text{total anion}] / [\text{total cation}]$: R_{ION} was in the 0.80-1.15 range in this observation

The two analytical quality tests above-mentioned indicated that pH and electric conductivity were measured accurately and that the major ions (Na^+ , K^+ , Ca^{2+} , Mg^{2+} , NH_4^+ , Cl^- , SO_4^{2-} , and NO_3^-) had also been analyzed with satisfactory accuracy.

3.3.2 Sea-Salt Constituent

Previous studies of acid rain in Japan (e.g., Fukuzaki *et al.*⁽⁵⁾; Wada *et al.*⁽⁶⁾; Hara⁽⁷⁾), has focused on the increases in the amounts of non-sea-salt SO_4^{2-} (hereafter, non-sea-salt is referred to as nss) in the atmospheric depositions that were sampled in the coastal areas along the Sea of Japan in winter. The increases have been attributed to the advection and transportation of contaminants from East Asia. On the other hand, some

problems have been noted with the methods used for making estimates of the sea-salt fraction in the atmospheric deposition (Garland⁽⁸⁾; Hiraki *et al.*⁽⁹⁾; Parungo *et al.*⁽¹⁰⁾).

The chemical composition of sea-salt particles generated by bubbles breaking on the sea surface is different from that of bulk seawater. Garland⁽⁸⁾ showed that the ion fractionation of sea-salt particles might occur during the particle formation at the sea surface and that the ratio of SO_4^{2-} to Na^+ in the spray exceeded that of seawater by 10 to 30 %. Many of the anomalous ion ratios of marine constituents of atmospheric aerosols and rain water are the result of ion enrichment in aerosols dispersed from bursting bubbles; nevertheless, the coefficients of the variations of $\text{SO}_4^{2-}/\text{Cl}^-$, Na^+/Cl^- , and $\text{Mg}^{2+}/\text{Cl}^-$ ratios of seawater in various oceans are less than 1 % (Horne⁽¹¹⁾).

Table 3.1 Relationship between $[\text{Na}^+]$ and the other major ion concentrations of wet atmospheric depositions.

Constituent	Correlation Coefficient	MR*	MR of Standard Sea Water
Cl^-	0.9998	1.18	1.18
SO_4^{2-}	0.9962	0.062	0.061
K^+	0.981	0.021	0.021
Mg^{2+}	0.9993	0.114	0.114
Ca^{2+}	0.993	0.023	0.023

*"MR" is the mole ratio of the other major ion concentration to $[\text{Na}^+]$.

Table 3.1 shows the relationship between $[\text{Na}^+]$ and the other major ion (K^+ , Ca^{2+} , Mg^{2+} , Cl^- , and SO_4^{2-}) concentrations of wet atmospheric depositions. The major ions are highly correlated with $[\text{Na}^+]$, and the mole ratios are in good agreement with those

of standard seawater as shown in Section 2 Figure 2.8. Therefore, it is thought that the chemical characteristics of sea-salt constituents changed little during the particle formation when seawater was sprayed out from the sea surface even though some modifications of the sea-salt constituents were observed in aerosol and snow (e.g., Okada *et al.*⁽¹²⁾; Gjessing⁽¹³⁾; Posfai *et al.*⁽¹⁴⁾; Hall⁽¹⁵⁾).

Total 46 atmospheric deposition samples were examined here, and the $[\text{Na}^+]$ of 37 samples was less than 1 mM. A low concentration sample is affected greatly by the anthropogenic pollutants than a high concentration sample. To examine the contribution of contaminants to atmospheric depositions, a magnified form figure of the relationship between $[\text{Na}^+]$ and the concentrations of the other major ions in a range of less than 1.0 mM is shown in Figure 3.2. Each line is a regression between the concentration of major ions and $[\text{Na}^+]$. Most of the constituents correlate well with Na^+ , except for SO_4^{2-} and K^+ . The concentrations of both constituents are 0.04 mM higher at the maximum than those of standard seawater. Therefore, we concluded that SO_4^{2-} and K^+ originated not only from seawater but also from some anthropogenic sources.

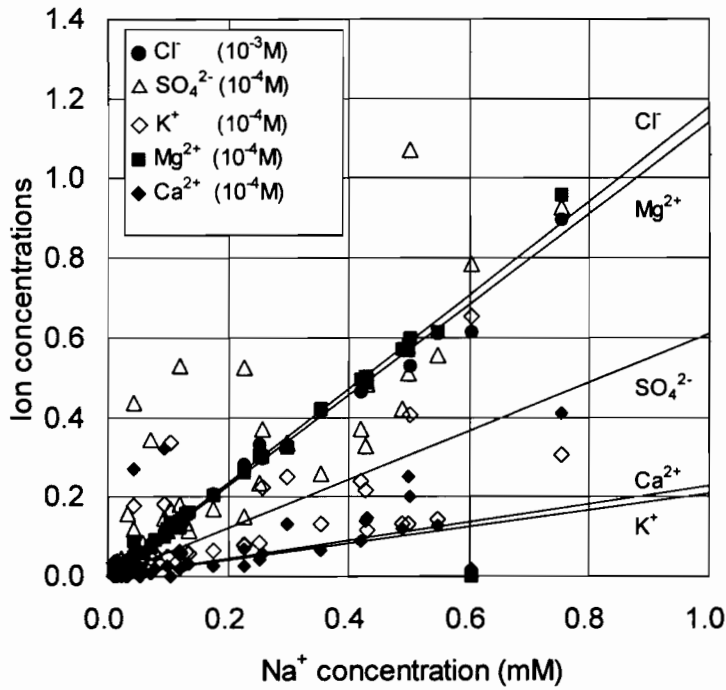


Figure 3.2 Relationship between $[\text{Na}^+]$ and the other major ion concentrations of wet atmospheric depositions. Solid lines are concentration of each constituents in standard seawater.

3.3.3 Origin of NO_3^-

Figure 3.3 shows the relationship between the atmospheric deposition amounts of Na^+ and NO_3^- and the rainfall amount based on 34 wet atmospheric deposition samples. The atmospheric deposition amounts are proportional to the amount of rainfall. The regression lines of both ions in the figure are as follows:

$$\text{Na}^+ \text{ depositions} = 0.50 \times (\text{rainfall})^{1.5} \quad (1)$$

$$\text{NO}_3^- \text{ depositions} = 0.01 \times (\text{rainfall})^{0.9} \quad (2)$$

As seen in the figure, the slope of the Na^+ atmospheric deposit is steeper than that of NO_3^- . If the deposit of NO_3^- originates from seawater, as does the Na^+ , the ratio of the deposit of NO_3^- to that of Na^+ should be constant. This means that both slopes should be identical and parallel each other. However, the slopes are not the same, and the deposition ratio of NO_3^- to Na^+ is not constant. Therefore, we conclude that NO_3^- did not originate from sea-salt but from anthropogenic activity on land. Fukuzaki and Oizumi⁽¹⁶⁾ described scavenging processes in which atmospheric depositions were governed by two processes called as “washout” and “rainout”, which are caused by rain and clouds, respectively. However, in this analysis it is not clear whether these processes contributed to the deposition of NO_3^- .

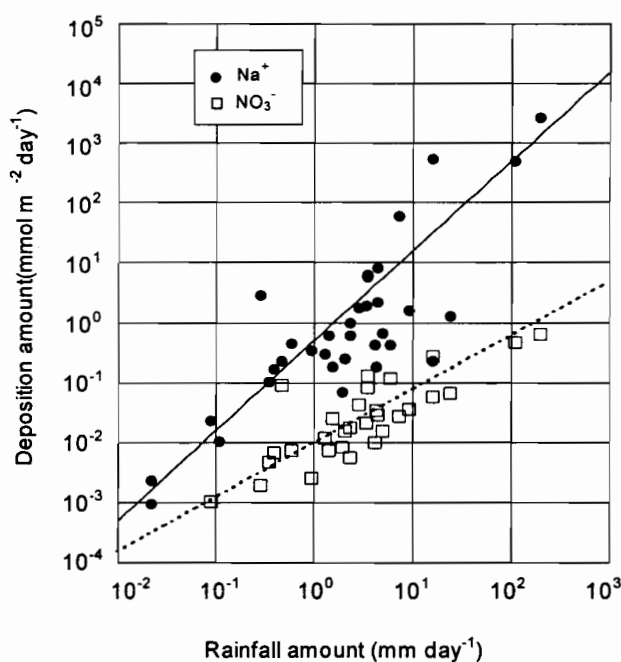


Figure 3.3 Relationship between the atmospheric depositions and rainfall.

3.3.4 Chemical characteristics

The cruise time series of $[H^+]$, $[Cl^-]$, $[NO_3^-]$, and $[nss-SO_4^{2-}]$ are shown in Figure 3.4. The abscissa axis is taken along the longitudes of the Yokohama-Vancouver-Honolulu-Tokyo cruise. The pH value ranged from 6.8 to 4.1 ($[H^+]$ is from 0.0001 to 0.1mM), and at 42N and 165W in the westerly wind zone the lowest pH value (pH=4.1) of the wet atmospheric deposition was observed to be similar to the result observed by Miyake *et al.*⁽²⁾ They found some special locations of high $[SO_4^{2-}]$ in the Central North Pacific Ocean. Except for the coastal areas near Japan and the United State of America, the pH of the dry atmospheric depositions was around 5.5. In the sea area of 35N and 150-175E, the pH was high, about 6-7, and in the sea area of 40-45N and 175-160W, the pH was low, less than 4.5.

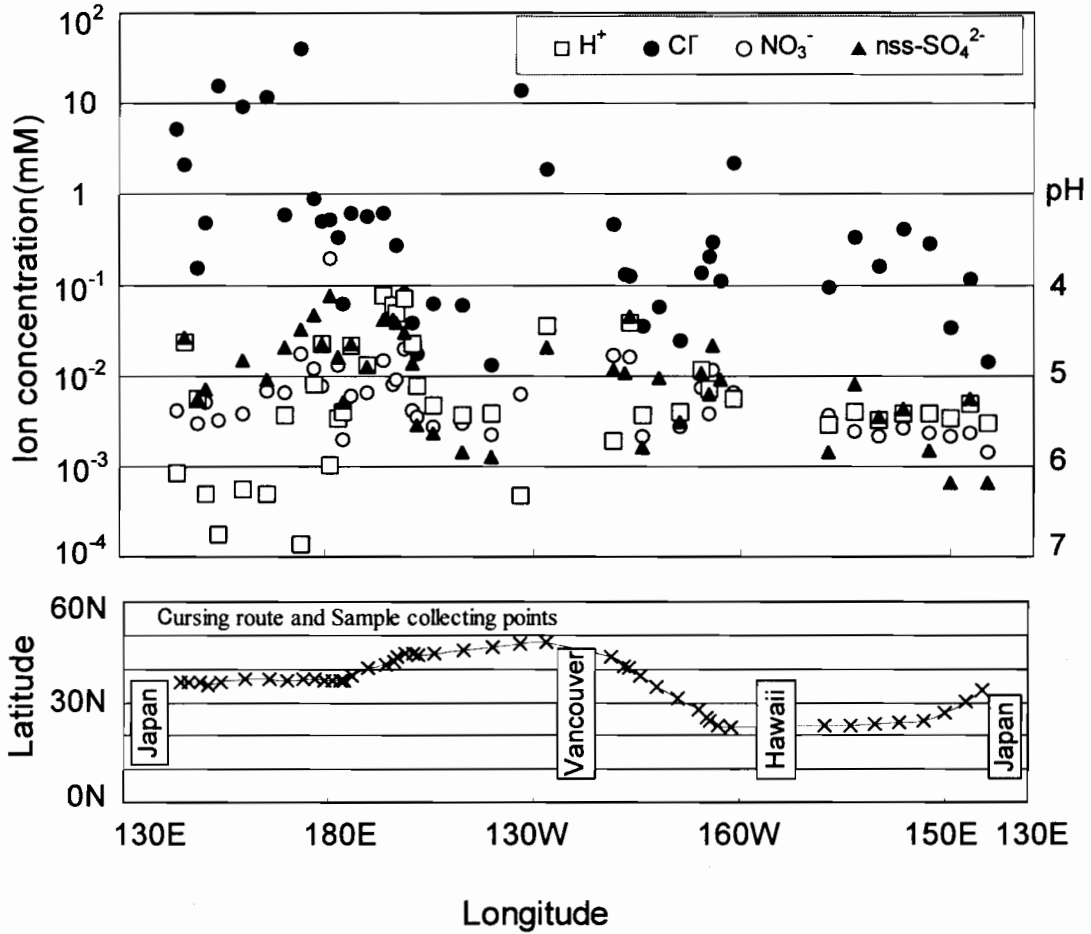


Figure 3.4 $[H^+]$, $[Cl^-]$, $[NO_3^-]$ and $[nss-SO_4^{2-}]$ along the longitude of the cursing route.

$$[nss-SO_4^{2-}] = [SO_4^{2-}] - 0.061 [Na^+]$$

As seen in Figure 3.4, $[nss-SO_4^{2-}]$ and $[NO_3^-]$ in the sea area of 35-50N in the westerly wind zone during the cruise from Yokohama to Vancouver were about 0.001 to 0.1 mM and 0.002 to 0.02 mM, respectively, higher than those in the sea area of 20-30N in the trade wind zone during the cruise from Vancouver to Tokyo via Honolulu. These constituents with high concentrations in the mid-latitude seas, compared to those in the low latitudes, are thought to affect the acidification of rainwater. As a general

feature, the variation in pH and ion concentration in the atmospheric depositions in the trade-wind zone is less than that in the westerly wind zone.

Sea-salts are thought to be major constituents of the atmospheric depositions over the open ocean far from land. The acidity of seawater is closely related to that of dissolved CO_2 ⁽¹⁷⁾, and the acidity of the atmospheric depositions is also governed by CO_2 . The $[\text{H}^+]$ of rainwater in equilibrium with the CO_2 concentration in the air is obtained as follows⁽¹⁾:

$$[\text{calH}^+] = 2.28 \times 10^{-9} D^{-1} + C, \quad (3)$$

$$D = 455 [\text{mesNa}^+]^{-1}, \quad (4)$$

$$C = 0.5 \{ -2.35 \times 10^{-3} D + [(2.35 \times 10^{-2})^2 - 2.144 \times 10^{-11} (D^{-2} - 1)]^{0.5} \}, \quad (5)$$

where $[\text{calH}^+]$ is the theoretically calculated H^+ concentration in mM and $[\text{mesNa}^+]$ is the measured Na^+ concentration in mM. The dilution factor D is obtained assuming that $[\text{CO}_2]$ in the diluted seawater is in equilibrium with $[\text{CO}_2]$ in air, the total carbon concentration in seawater is $12 \mu\text{M}$, and $[\text{Na}^+]$ in seawater is 455 mM. C is the correction factor of $[\text{calH}^+]$ due to the effect of $[\text{CO}_2]$ in air and estimated from the dilution factor D .

To clarify the acidification constituents of the atmospheric depositions in the observation sea, the difference between $[\text{mesNa}^+]$ and $[\text{calH}^+]$ ($\Delta[\text{H}^+]$; $\Delta[\text{H}^+] = [\text{mesH}^+] - [\text{calH}^+]$) is shown in Figure 3.5 against the nss-ion concentration ($[\text{nss-ion}] = [\text{NO}_3^-] + 2[\text{nss-SO}_4^{2-}] - [\text{nss-NH}_4^+] - [\text{nss-K}^+] - 2[\text{nss-Mg}^{2+}] - 2[\text{nss-Ca}^{2+}]$). The difference is proportional to $[\text{NO}_3^-] + 2[\text{nss-SO}_4^{2-}]$. Therefore, we concluded that these ions contribute as acidification constituents in the atmospheric depositions. Although the nss-cation

concentrations were quite low, these cations contribute to neutralize the atmospheric depositions.

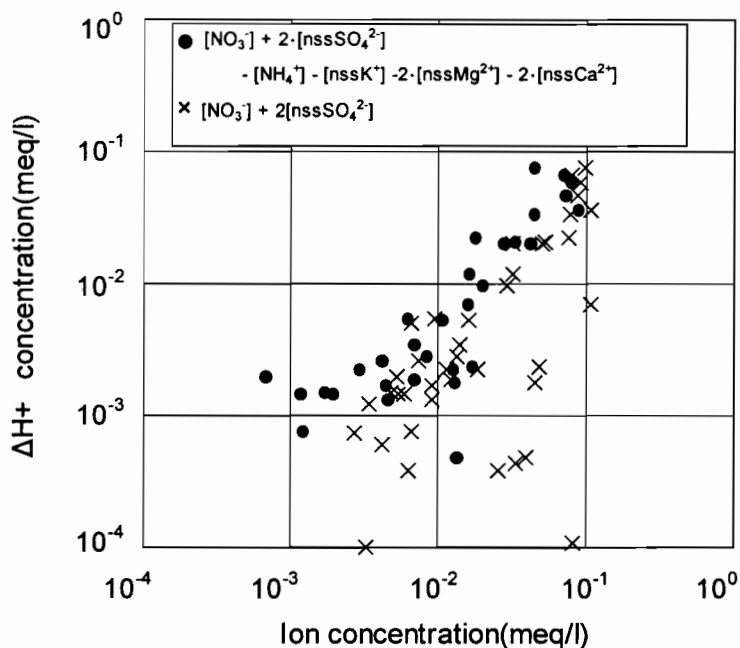


Figure 3.5 Relationship between $[\Delta H^+]$ and the nss-ion concentration.

$$[\Delta H^+] = [_{mes}H^+] - [_{cal}H^+].$$

$[_{mes}H^+]$ is the measured $[H^+]$, and $[_{cal}H^+]$ is the theoretically calculated $[H^+]$.

3.4 Conclusion

The investigation of wet and dry atmospheric depositions was carried out on board of the T/S Nippon Maru, a tall sailing ship, from June 22 to August 28, 1992, over the North Pacific Ocean. Although the main constituents of the atmospheric depositions originated from sea-salt constituents, the pH value of the wet depositions was in the 4.1-6.8 range and was lower than the pH of seawater. The atmospheric depositions in the

mid-latitude seas of the westerly wind zone were as strongly acidified as they are in urban areas.

Although there was no source of anthropogenic pollutants in this area, $[\text{nss-SO}_4^{2-}]$ and $[\text{NO}_3^-]$ in the atmospheric depositions were higher than they were in the lower latitudes of the trade-wind zone. These constituents were generally considered to have originated in East Asia. However, we were not able to determine any tendency in attenuation relative to the distance from Japan. However, in the low latitudes of the sea in the trade-wind zone, the constituent concentrations of the atmospheric depositions were low, and they changed very little.

$[\text{H}^+]$ in diluted seawater was calculated theoretically and compared with the measured $[\text{H}^+]$. The difference was related to the ion balance of the nss-constituents. We concluded that nss-SO_4^{2-} and NO_3^- were acidification constituents and that nss-cations were neutralization constituents.

References

- (1) Hiraki, T., H. Ishida, and M. Hayashi (2000): Measurement of the Atmospheric Deposition over the Western Pacific Equatorial Ocean, *Marine Meteorol. Soc., Sea and Sky*, 76, 2, 119-124.
- (2) Miyake, H., J. Sasaki, T. Iwao, K. Oda, T. Yamauchi, T. Inoue, N. Shiota, and H. Tsubo (1993): Long-range Transport of Aerosol over the North Pacific Ocean, *Nuclear Instruments and Methods in Phys. Res.*, B75, 282-286.
- (3) Hiraki, T., M. Tamaki, M. Shoga, H. Ishida, T. Iwao, and Y. Nakamura (1993): On-board Measurements of Atmospheric Deposition over the North Pacific Ocean, *Rep. of the Hyogo Prefectural Institute of Environ. Sci.*, 25, 20-25. (in Japanese)
- (4) The Research Group of Acid-rain Investigating Method (1993): Acid Rain Investigation Method, Gyousei, pp.183. (in Japanese)
- (5) Fukuzaki, N., T. Oshio, I. Noguchi, M. Matsumoto, S. Morizaki, M. Oohara, M. Tamaki, and T. Hiraki (1996): Chemical Features of the Major Constituents in Winter Precipitation along the Sea of Japan on Honshu Island, Japan, *J. Chem. Soc. Japan*, 8, 726-733. (in Japanese)
- (6) Wada, A., T. Miyao, and Y. Dokiya (1997): Chemical Components of the Precipitation in Relation to Meteorological Elements, *Marine Meteorol. Soc., Sea and Sky*, 72, 3/4, 81-92. (in Japanese)

- (7) Hara, H. (1997): Precipitation Chemistry in Japan, *J. Chem. Soc. Japan*, 11, 733-748.
(in Japanese)
- (8) Garland, J. A. (1981): Enrichment of Sulphate in Marine Aerosols, *Atmos. Environ.* 15, 5, 787-791.
- (9) Hiraki, T., M. Tamaki, and Y. Torihashi (1988): Influence of Sea-salt Particles on Atmospheric Pollutant Deposition, *Rep. of the Hyogo Prefectural Institute of Environ. Sci.*, 20, 13-22. (in Japanese)
- (10) Praungo, F., C. Nagamoto, M. Y. Zhou, and N. Zhang (1992): Wet and Dry Deposition of Atmospheric Aerosols in the Pacific Ocean, the Fifth Intern. Conference on Precipitation Scavenging and Atmospheric-surface Exchange Processes, 2, 867-881.
- (11) Horne, R. A. (1969): *Marine Chemistry*, Wilkey Interscience, New York.
- (12) Okada, K., Y. Ishizaki, T. Masuzawa, and K. Isono (1978): Chlorine Deficiency in Coastal Aerosols, *J. Meteorol. Soc. Japan*, 56, 501-507.
- (13) Gjessing, Y. (1989): Excess and Deficit of Sulfate in Polar Snow, *Atmos. Environ.*, 23, 1, 155-160.
- (14) Posfai, M., J. R. Anderson, P. R. Buseck, T. W. Shattuck, and N. W. Tindale (1994): Constituents of Remote Pacific Marine Aerosols: A TEM Study, *Atmos. Environ.*, 28, 10, 1747-1856.

- (15) Hall, J. S., and E. W. Wolff (1998): Causes of Seasonal and Daily Variations in Aerosol Sea-salt Concentrations at a Coastal Antarctic Station, *Atmos. Environ.*, 32, 21, 3669-3677.
- (16) Fukuzaki, N., and T. Oizumi (1995): Scavenging Processes as Revealed by Dependence of Wet-deposition of Chemical Species on Precipitation Amount, *J. Environ. Sci. Japan*, 8, 4, 425-430. (in Japanese)
- (17) Lewis, E., and D. Wallace (1998): Program Developed for CO₂ System Calculations, ORNL/CDIAC-105, Carbon Dioxide Information Analysis Center, Oak Ridge National Laboratory, U.S. Department of Energy.

Chapter 4

Seasonal Variation of Atmospheric Ozone Concentration over the Western Pacific

4.1 Introduction

Ozone plays an important role of acidifying atmospheric deposition as well as shutting off harmful ultraviolet rays and the global warming in the global environmental issues. In recent years, the increasing of the ozone concentration in the troposphere has been pointed out⁽¹⁾ and many researches have been reported to support the trend (e.g, Monks⁽²⁾, Thompson *et al.*⁽³⁾, Pochanart *et al.*⁽⁴⁾, Japan Meteorological Agency⁽⁵⁾). The altitudinal distribution of the ozone concentration is regularly monitored by the Japan Meteorological Agency. The typical ozone layer has about 20km thickness and the maximum peak of the concentration is observed at an altitude of 20-30km with the partial pressure 15mPa. The altitude of the highest partial pressure of ozone was found to be low in high latitudes. In Sapporo in the high latitude, the highest partial pressure was observed in the altitude of 20-24km while in Naha in low latitudes it was done 24-28km.

Ozone is generated in the stratosphere and transported to high latitudes by the Brewer-Dobson circulation and precipitate in the troposphere in high latitudes. This transportation from the tropical zone to high latitudes becomes active in winter, and thus ozone is accumulated in high latitudes in the period from winter to spring. Many investigations have showed the maximum concentration of tropospheric ozone in spring in the northern hemisphere. Kim *et al.*⁽⁶⁾ studied the observational data of rawinsondes, ozonesondes and TOMS of the satellite. They found that the gradients of potential temperature and isentropic vorticity near the upper troposphere over Korea were steeply sloping. It was regarded that ozone of upper level over east Asia penetrated into the lower level or ground over Korea because of the downstream due to tropopause folding near the jet streams and the sinking of surface high pressure.

Kirchhoff⁽⁷⁾ mentioned that the ozone maximum near the equator was caused by biomass burning. Cros *et al.*⁽⁸⁾ also showed the ozone maximum in Africa in September when biomass burning was most frequently done. Crutzen and Andreae⁽⁹⁾, Levine⁽¹⁰⁾, and Hudson and Thompson⁽¹¹⁾ estimated the influence of forest and savanna fire on the tropical tropospheric ozone and suggested a global-scale influence of biomass burning especially over the Atlantic region based on the satellite data.

To show the global background concentration and its distribution trends of the ozone concentration in the surface atmosphere in the western Pacific Ocean, the result and analysis of the atmospheric ozone concentration measured on board during the cruises between Japan and Australia from 1993 to 1998 are detailed in this paper.

4.2 Observation and Analytical Method

As listed in Table 4.1, the atmospheric ozone concentration was measured on board during one-month long cruises between Japan and Australia every August (hereafter refers to “summer cruise”) from 1993 to 1998 and from January 23rd to March 2nd in 1998 (mainly in February, hereafter refers to as “winter cruise”). Figure 4.1 shows the cruising routes of the cruises between Japan (Kobe) and Australia. To avoid the atmospheric pollution, no samples were taken when arriving at and leaving the ports.

Table 4.1 Outline of observational cruises

Cruise	Cruising route	Period
1	Kobe - Freemantle	12 Aug. – 10 Sep. 1993
2	Kobe - Freemantle	14 Aug. – 10 Sep. 1994
3	Kobe - Freemantle	13 Aug. – 10 Sep. 1996
4	Kobe - Freemantle	11 Aug. – 9 Sep. 1997
5	Kobe - Brisbane	23 Jan. – 2 Mar. 1998
6	Kobe - Freemantle	12 Aug. – 10 Sep. 1998

Summer cruise measurements were made on board the P/S Orient Venus of Nihon Cruise Co., Ltd. The winter cruise measurement was conducted on board the T/S Hokuto Maru of National Institute for Sea Training, Independent Administrative institution. The atmospheric ozone concentration was measured continuously by the ultraviolet photometric method (*Daishibi* 1006AHJ). Samples were taken every one

minute. The hourly mean is used for the analysis here. Sampling air was intaken from the height of about 20m above the sea level through the teflon tube.

To study the origin of ozone in the surface atmosphere, the back trajectory analysis of the air mass was performed by using the air mass trajectory analysis, the “Cger-Gmet” system developed by Hayashida *et al.*⁽¹²⁾ and improved by Katsumoto⁽¹³⁾. The meteorological data set issued by European Centre for Medium-Range Weather Forecasts was applied as the basic data. The back trajectory(latitude, longitude and altitude) was calculated by tracing the air mass every six hours for the last five days using the isentropic method starting from the altitude of 1200m.

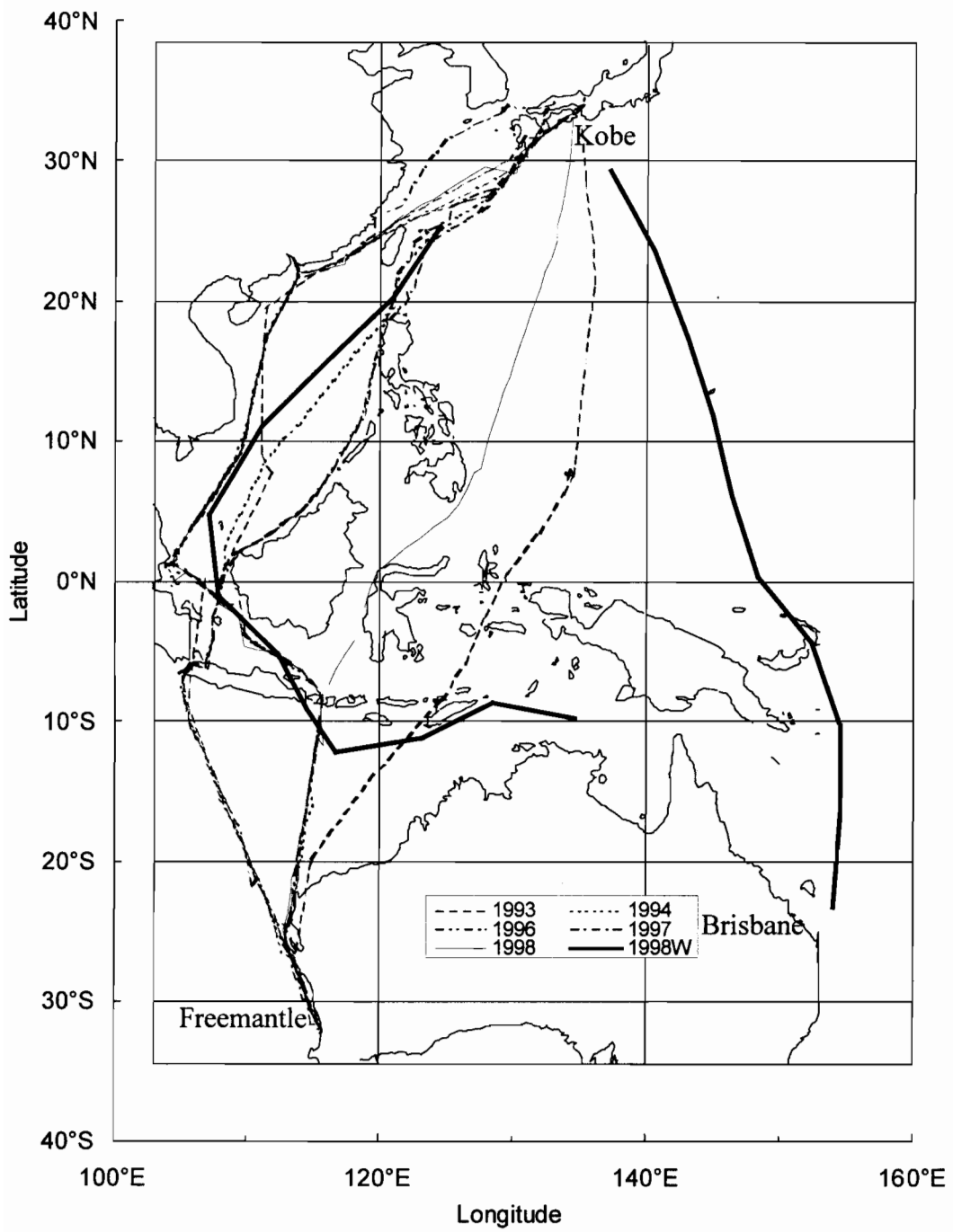


Figure 4.1 Cruising routes of observational ships.

4.3 Result and Discussion

4.3.1 General feature of Ozone Concentration

In summer the ozone concentration on the sea ranged from about 0 to 37.5ppbv and the average for five years was 17.4ppbv. In winter the concentration was about 10 to 60.9ppbv and the average was 28.3ppbv. In urban areas, the ozone concentration has a maximum peak in the afternoon⁽¹⁴⁾ because of the photochemical reaction. But as reported by Laat⁽¹⁵⁾, the diurnal variation was observed only several ppb over the sea.

Figure 4.2 is the time series of the ozone concentration in the summer cruise from August 13 to September 10, 1996(upper figure) and the winter cruise from January 23 to March 2, 1998(lower figure). The solid circle in the figure shows the hourly average. As a whole, there were no significant diurnal variations, but the gradual change was observed. However, there were some exceptional changes of the concentration. The positions and days which had concentration change abruptly are as follows; the East China Sea on August 13-14, near the Philippines on September 6, near Papua New Guinea on January 30 and Indonesia on February 18. In these areas, the ozone concentration seemed to be affected by air pollutants from the anthropogenic activities.

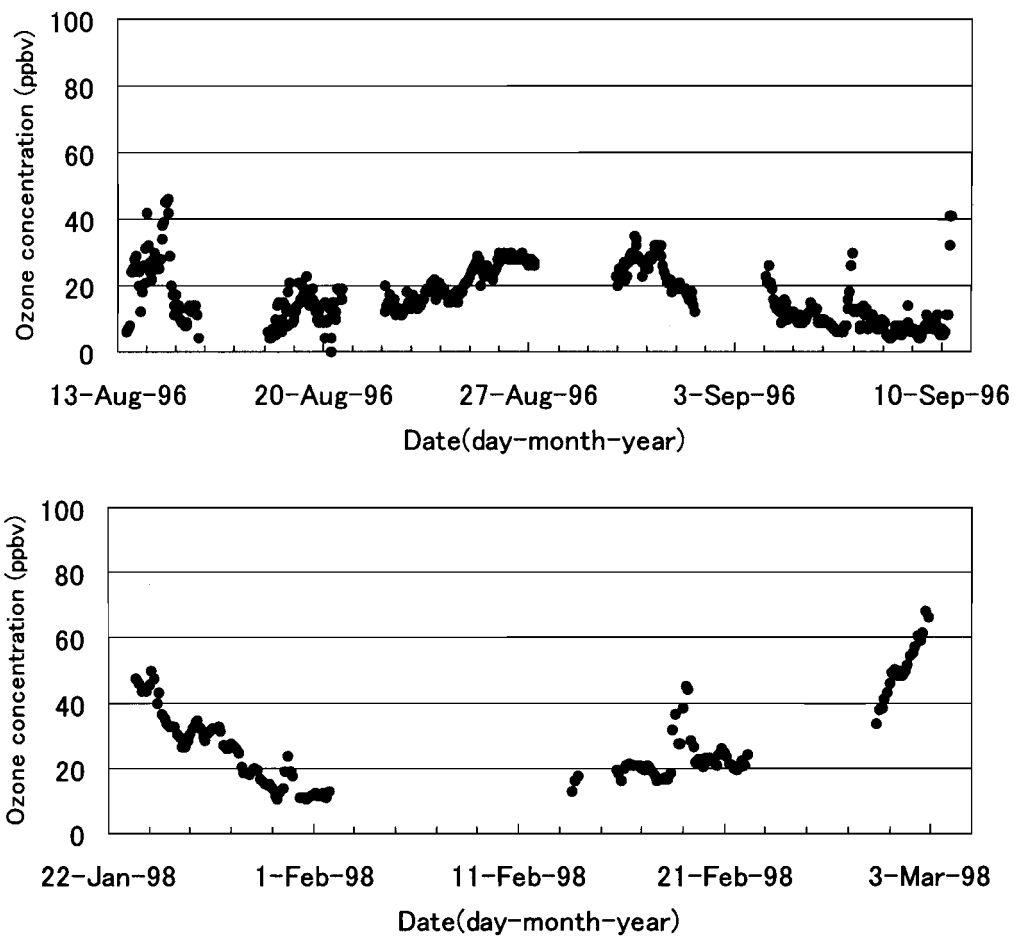


Figure 4.2 Time series of the ozone concentration in summer and winter cruises.

4.3.2 Meridional distribution of Ozone Concentration

The observation of the ozone concentration was made in the meridional zone between 110 to 150 degrees E and the cruise was made mostly along the meridional direction in that zone. Thus, the time variation of the ozone concentration can be converted to the meridional variation. Although there is about one-month difference in the observing time, the effect of this sampling time difference might be negligible because no significant difference was recognized between both ozone concentrations at leaving and arriving at Japan. Figure 4.3 shows the meridional distribution of the ozone concentration. Figs. 4.3 (A) and (B) are the observational results of 5 summer cruises for 5 years and one winter cruise, respectively. They show every 10-degree latitudinal average(solid circle), median(open circle) and one standard deviation(bar) of the ozone concentration.

The ozone concentration in 30 degrees N showed a large variation because of some exceptional high values. The average concentration was 15ppbv and higher than the median of 12.0ppbv. The median was almost the same as 11.8ppbv at 20 degrees N. Hereafter, the median is used for the analysis and discussion because the average contained some exceptional large changes and values in the observational data.

The ozone concentration in summer was about 12ppbv, 19ppbv and 27ppbv in 20-30 degrees N, near the equator and in 20-30 degrees S, respectively. The concentration tends to decrease northward along the latitude from 30S to 20N. The concentration in winter was about 11ppbv, 22ppbv and 41-47ppbv in 20 degrees S, near the equator and 20-30 degrees N, respectively. The concentration showed a clear increasing tendency

northward contrary to the northward decreasing tendency of the ozone concentration in summer.

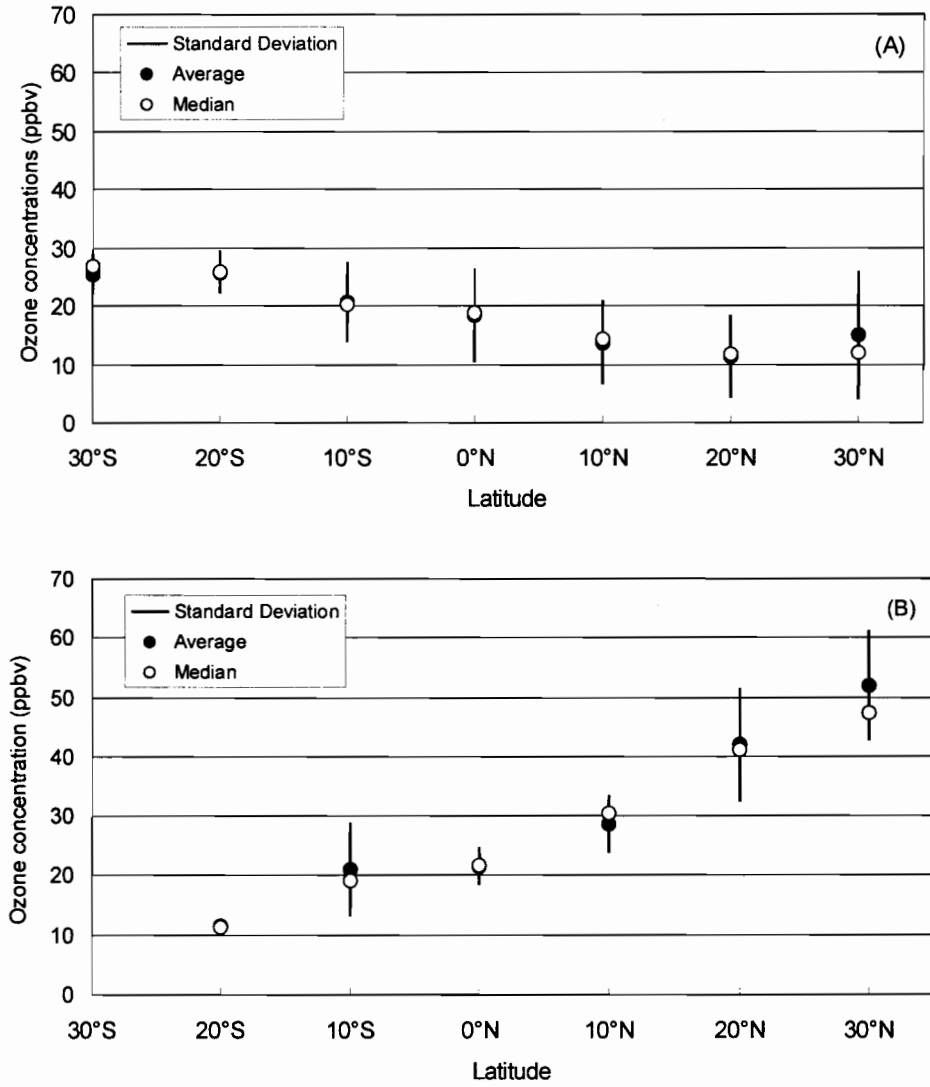


Figure 4.3 Meridional distribution of ozone concentration.

Figures (A) and (B) are the results from the data of summer cruises in 1993,1994,1996,1997, and 1998 and the data of the winter cruise in 1998, respectively. The solid and open circles show every 10-degree latitudinal average and median, respectively. The bar shows one standard deviation.

4.3.3 Seasonal Variation of Ozone Concentration

The seasonal variation of the ozone concentration is known that a smaller change is observed in low latitudes, while a larger change is found in high latitudes⁽⁶⁾. In our measurement, the ozone concentration near the equator was almost same and about 20ppbv in both seasons. But in 30 degrees N the concentration in winter was 47ppbv and 4 times higher than that in summer(12ppbv). In 20 degrees N the concentrations in winter and summer were 41ppbv and 12ppbv respectively, and the difference was a little smaller than that in 30 degrees N. Similarly, in 10 degrees N the concentrations in winter and summer were 31ppbv and 14ppbv respectively. The difference was smaller than that in 20 and 30 degrees N. In the equator and 10 degrees S, the concentrations in winter and summer were the nearly same concentration of 21ppbv. In 20 degrees S, the concentrations in winter and summer were 11ppbv and 26ppbv respectively. The concentration in winter is about half of that in summer, but the difference, 14ppbv, is smaller than 29ppbv in 20 degrees N. In the mid latitudes, the seasonal variation was the smallest among those observed.

Pocharart *et al.*⁽¹⁶⁾ analyzed the observational data from 1994 to 2000 in Rishiri, Oki, Okinawa and Ogasawara islands in Japan. They showed the common trend in these four isolated islands that the concentration showed the maximum in spring and the minimum in summer. The low concentration was caused by the oceanic air mass. In summer(from June to August), the concentration was 15ppbv and 13ppbv in Okinawa and Ogasawara islands, respectively. The air pollution transported from main island of Japan affected to the ozone concentration at Oki and Rishiri and the concentrations were 40ppbv and 32ppbv respectively. In winter (from December to February), the anthropogenic air pollution in East Asia and the photochemical reaction influenced the

concentration and the concentration was 40ppbv in Rishiri and Ogasawara. The concentrations in Oki and Okinawa were 44ppbv and 46ppbv. The difference of the concentration among these islands was smallest in winter. In our results obtained near Japan, the variation of the ozone concentration in winter was as large as that in summer. This was different from their measurement result in the island in Japan by Pochartart *et al.*⁽¹⁶⁾. However, the seasonal tendency of low concentrations in summer and high concentrations in winter were in agreement with their results. It was concluded that the seasonal tendency was different characteristics of the ozone concentration in the surface atmospheric boundary layer in the Western Pacific Ocean.

Fujiwara *et al.*⁽¹⁷⁾ revealed the seasonal variation of tropospheric ozone in Indonesia based on 5-year ground-based observations. In the rainy season(from December to March), the ozone concentration in the surface atmosphere was constant and about 25ppbv. The standard deviation of the ozone concentration in each altitude was less than 10ppbv. In the dry season(from August to November), the concentration was as high as 40ppbv and showed the maximum 45ppbv in the middle layer of the troposphere and decreased vertically to about 25ppbv in the upper layer of the troposphere. Thompson *et al.*⁽¹⁸⁾ showed that tropospheric ozone over the Indian Ocean and the Pacific Ocean was well affected by the El Nino phenomena from 1997 to 1998 and the contamination material was transported from Africa based on the data of SHADOZ(the Southern Hemisphere Additional Ozonesondes) network. This study includes the same observation sites in Indonesia. Both rainy and dry seasons were included in this research, but no high concentration was observed near the equator in the dry season and no significant change between seasons was found.

4.3.4 Seasonal Characteristics of Meteorological Elements and Ozone

Concentration

The biggest difference among the meteorological elements in summer and winter is solar radiation. As a result the thermal distribution was inverted in northern and southern hemispheres. And in accordance with the thermal inversion in the global scale, the wind direction was also inverted in this area. Figure 4.4 shows the wind rose based on every 4-hour data in the summer cruise in 1996 and in the winter cruise in 1998. In summer southerly winds were prevailing, while in winter northerly winds were prevailing. Taking a consideration of the meridional distribution of the ozone concentration in summer, the ozone concentration showed an increasing tendency windward in the southern hemisphere and a decreasing tendency leeward in the north hemisphere. The similar tendency was observed in winter; the high concentration in the windward in the north hemisphere and the low concentration in the leeward in the south hemisphere.

Based on the results at Cape Grim, Australia, Monks *et al.*⁽¹⁹⁾ pointed out that in the unpolluted air in the remote marine boundary layer the photochemical reaction leads to the net destruction of ozone. This destruction thought to be balanced by entrainment of ozone into marine boundary layer from the lower free troposphere. In the observation from January to February, the destruction rate of ozone was 1.2ppbv/day and 87% of the ozone loss. In the observation from August to September, the rate of 0.6ppbv/day and 64% of the ozone loss. As a source of ozone, in summer, the photochemical reaction was only 0.56ppbv/day, and thus the inflow of 2.1ppbv/day from the lower free troposphere was 79% of the ozone entrainment. In winter the entrainment rate by the photochemical reaction was as small as 0.29ppbv/day but the entrainment rate to the

lower tropospheric layer was further smaller and 0.1ppbv/day. Thus, the ozone entrainment by the photochemical reaction was 74% of the ozone entrainment. But there was a net imbalance between the production and destruction of ozone in the southern marine boundary layer. In summer the imbalance was +1.3ppbv/day and in winter was -0.6ppbv/day. And they thought that a large amount of uncertainty in these budgets must exist in the entrainment parameterization.

Based on the observation in August, the concentration decreased 3.25ppbv every 10degrees toward the north. During the observational period, the air mass moved 8 degrees for 5 days. Assuming that the transport speed of the air mass was same to that of the general air flow, the meridional distribution of ozone concentration was converted to the destruction rate of the ozone concentration. The destruction rate of the ozone concentration was 0.52ppbv/day and showed the similar value as the imbalance of Monks *et al.*⁽¹⁹⁾.

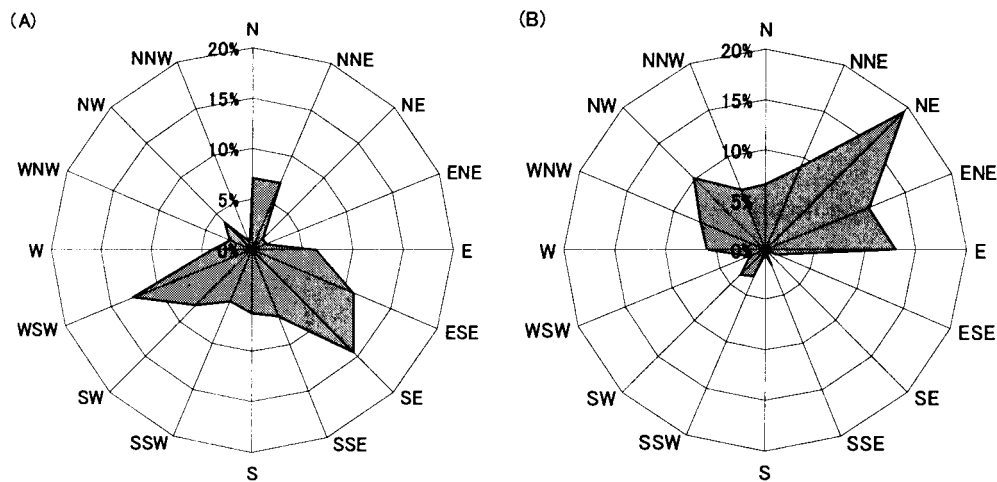


Figure 4.4 Wind rose in summer and winter cruises.

Figures (A) and (B) are the results from the data of cruises from August 13 to September 10 in 1996 and from January 23 to March 2 in 1998.

4.3.5 Air Mass Trajectory Analysis

The altitudinal distribution trend of the ozone concentration was widely and generally accepted. According to the ozone report by the Japan Meteorological Agency, Ozone Layer Observation Report 2001, the altitude of the highest concentration was lower in the higher latitudes; 20-24km(the height of about 50–30hPa) in Sapporo in the high latitude; 24-28km(the height of 15-30hPa) in Okinawa in the low latitude. In high latitudes, the ozone partial pressure has a seasonal change. The altitudinal distribution of tropospheric ozone was reported by Fujiwara *et al.*⁽¹⁷⁾ and Thompson *et al.*⁽¹⁸⁾. Monks *et al.*⁽¹⁹⁾ also suggested that tropospheric ozone originated from the inflow of the low free troposphere to the marine atmospheric boundary layer. Therefore, the altitudinal distribution of tropospheric ozone has an important role to govern the ozone concentration in the marine atmospheric boundary layer.

Pochanart *et al.*^(4,16,20) and Chan *et al.*⁽²¹⁾ used the air mass back trajectory to analyze the ozone concentration and showed the ozone concentration trend depending on its air mass origin. The low ozone concentration of the marine air mass was found to be common in their research. Broennimann *et al.*⁽²²⁾ studied the vertical distribution of the ozone concentration from 490m to 3600m above the sea level in Switzerland and showed the ozone concentration difference was attributed to the altitude of the air mass trajectory. Cooper and Peterson⁽²³⁾ also made a research in Washington State, U.S.A., and proved that the weekly average of the ozone concentration was dependent on the altitude of the air mass route.

In this research, the concentration was found to tend to decrease leeward. To further study the origin of ozone, the back trajectory analysis^(12,13) of the air mass was performed. Total 80 data sets in the summer cruise in 1996 and the winter cruise in

1998 were analyzed. The starting point for the air mass trajectory analysis was at the altitude of 1200m and the air mass history was traced for 5 days. The result is shown in Figure 4.5. From January 25 to February 1, air mass flow from the central part of the Pacific was seen. From February 16 to 21, some irregular winds blew. Air mass flow from the Chinese continent was observed, too. The trajectory of the air mass along the meridian in summer and winter cruises are given in Figure 4.6. As seen in Figure 4.6 (A), in summer, the air mass from the high latitudes in the southern hemisphere has its origin in high altitudes. As seen in Figure 4.6 (B), in winter, the air mass from the high latitudes in the northern hemisphere flowed down from high altitudes. In summer and winter, the general wind directions were opposite to each other. Figure(A) showed that the air mass from the high altitude flowed from the high latitudes in the southern hemisphere and Figure(B) showed that the air mass from the high altitude flowed from the high latitudes in the northern hemisphere. The relation between altitudes and latitudes of air masses was reversed in summer and winter. This was similar to the general trend of the wind direction in summer and in winter as described in the previous section.

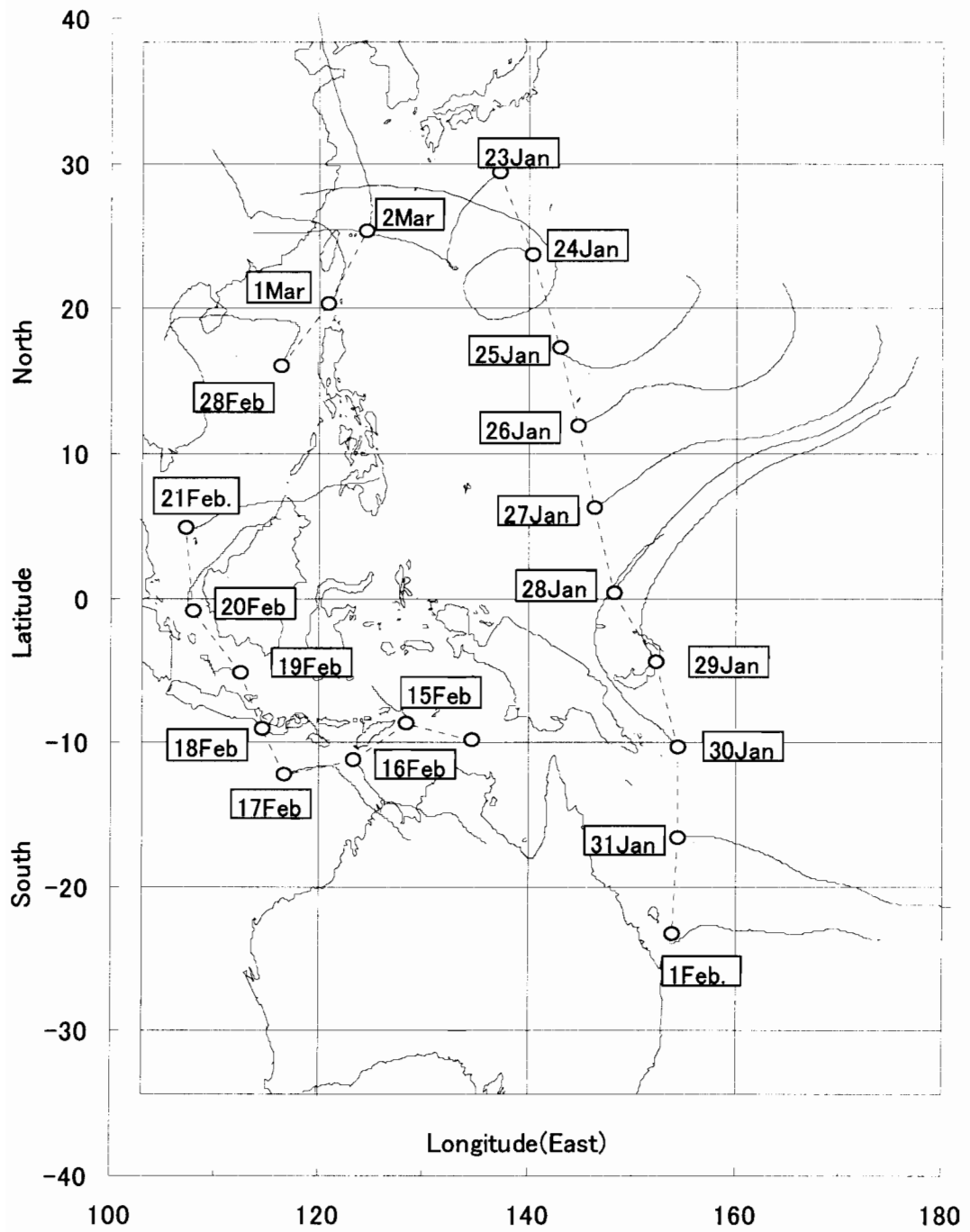


Figure 4.5 Air mass back trajectory analysis of the winter cruise in 1998.

The trajectory is shown for 5 days.

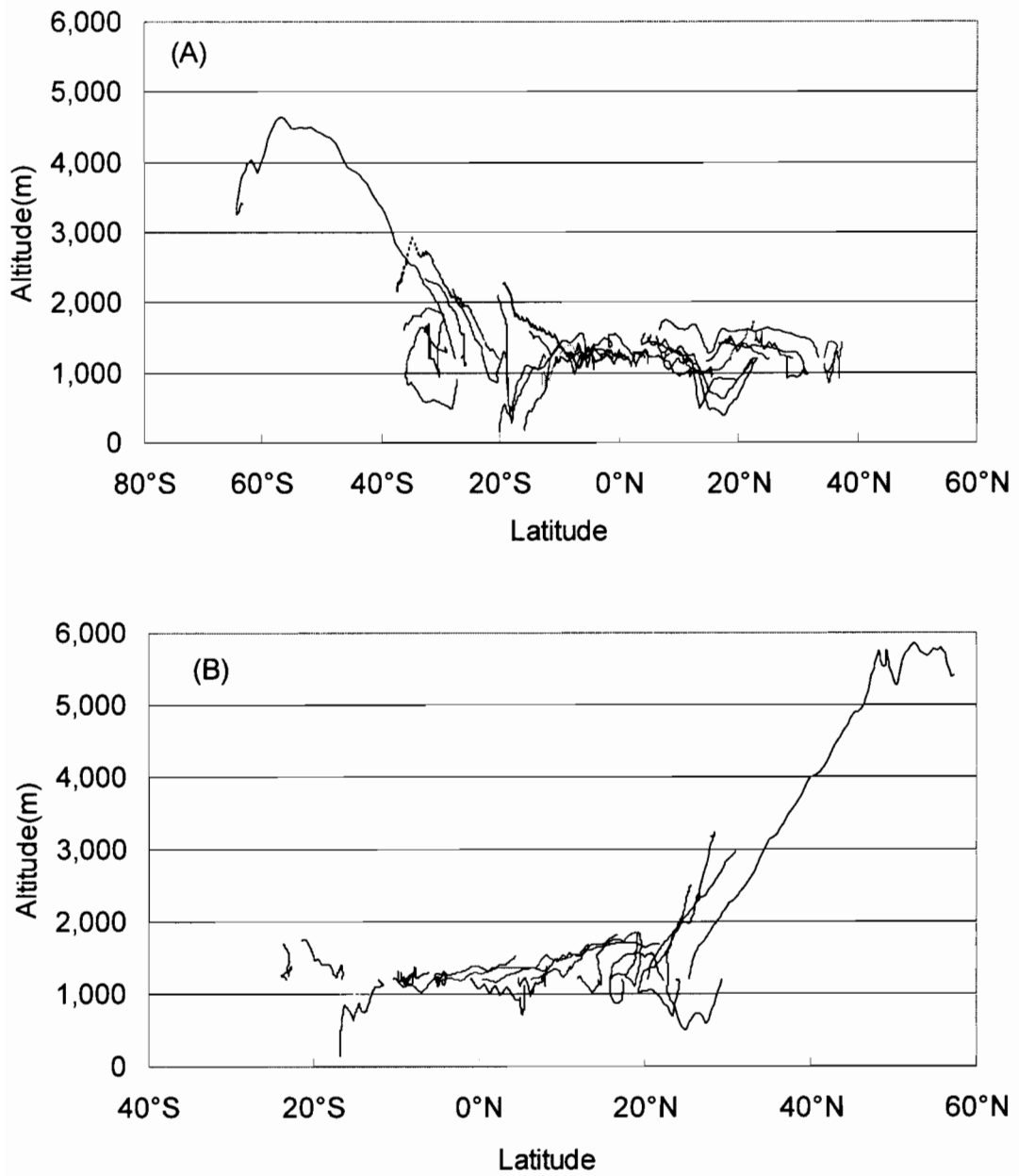


Figure 4.6 Air mass trajectory along the latitude.

Figure (A) and (B) show the air mass trajectory along the meridian based on the data of the summer cruise in 1996 and the winter cruise in 1998, respectively.

Figure 4.7 shows the relationship between the ozone concentration and the maximum passing altitude of the air mass trajectory in summer and winter. In summer, the maximum passing altitude of the air mass in five days was in the range of 1104-4640m. The ozone concentration of the air mass from the altitude of 1104m was as low as 11ppbv. The ozone concentration of the air mass passing through the altitude of 4640m was 28ppbv. The figure shows the good relationship between the ozone concentration and the maximum passing altitude of the air mass. The concentration was proportional to the maximum altitude.

In winter cruise, the concentration was higher than that in summer cruise. The daily average of the ozone concentration was in the range of 12ppbv-61ppbv. The maximum passing altitude of the air mass in five days was in the range of 1138m-5791m. The ozone concentration of the air mass passing through the altitude of 1138m was as low as 18ppbv, while the maximum passing altitude of the air mass passing through the altitude of 5791m was as high as 60.9ppbv. Similarly to the result in the summer cruise, in the winter cruise the ozone concentration of the air mass was proportional to the maximum passing altitude. These results were in good agreement with them by Broennimann *et al.*⁽²²⁾ and Cooper and Peterson⁽²³⁾. The global background concentration over the ocean was changed by the transportation of the air mass of the higher ozone concentration in the free troposphere than that on the ground level.

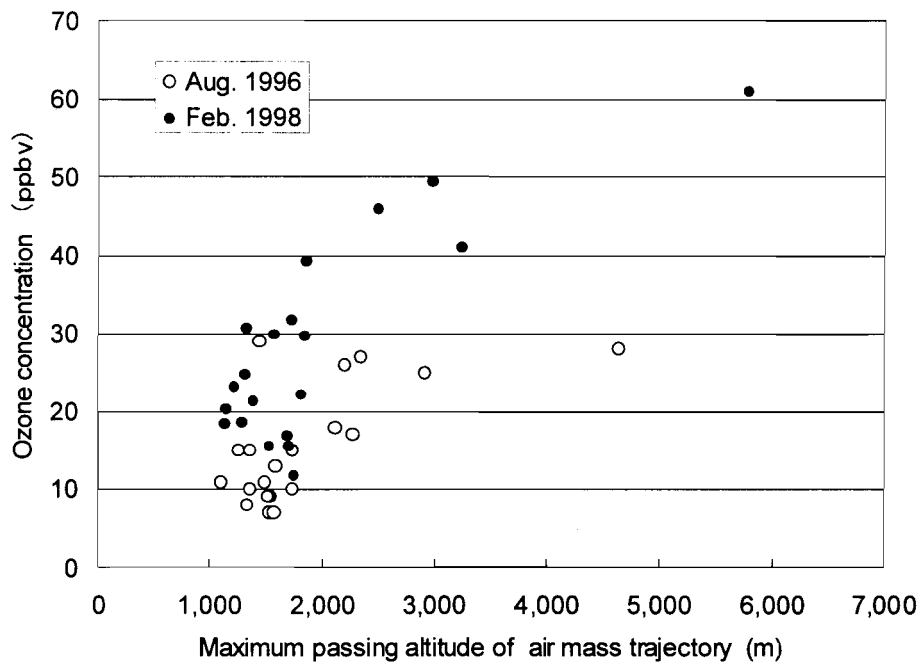


Figure 4.7 Relationship between the ozone concentration and the maximum passing altitude of the air mass trajectory.

The open and solid circles show the data in summer cruise in 1996 and winter cruise in 1998, respectively.

4.4 Conclusion

Ozone plays an important role as acidifying atmospheric depositions as well as shutting off harmful ultraviolet rays and the global warming effect in the global environment. In recent years, the increase of tropospheric ozone concentration has been pointed out. To unveil the characteristics of ozone in surface atmosphere in the Western Pacific Ocean, the atmospheric ozone concentration was measured during one-month cruises between Japan and Australia every August from 1993 to 1998 and from January 23 to March 2 in 1998.

The concentration measured over the sea was constant and the significant diurnal variation was not observed. In summer cruises, the ozone concentration in 30 degrees N was about 12ppbv and showed an increasing trend southward to the equator, where the concentration was about 19ppbv. In the southern hemisphere, the similar increasing tendency was observed southward. The concentration was almost 27ppbv in 30 degrees S. In winter, the ozone concentration increased northward contrary to the southward increasing tendency in summer. The concentration was 51ppbv in 30 degrees N, decreased to 22ppbv on the equator and further decreased to 11ppbv in 20 degrees S.

In this observational sea area, southerly winds blew generally in summer and northerly winds in winter. The meridional distribution of the ozone concentration was depending on the change of the general wind direction. The ozone concentration decreased leeward along the general wind.

To study the route of the air mass, the back trajectory analysis of the air mass was performed. Initial altitude of the back trajectory analysis was 1200m and the air mass history was traced for 5 days. The maximum passing altitude of air mass was 6000m.

It was found out that the ozone concentration of the air mass was well proportional to the maximum passing altitude of the air mass trajectory.

Reference

- (1) Guicherit, R. and M. Roemer (2000) : Tropospheric ozone trends, *Chemosphere Global Change Sci.*, 2(2), 167-183.
- (2) Monks P.S.(2000): A review of the observations and origins of the spring ozone maximum, *Atmospheric Environment*, 34, 3545-3561.
- (3) Thompson A.M., J.C. Witte, R.D. Hudson, H. Guo, J.R. Herman, M. Fujiwara(2001): Tropical tropospheric ozone and biomass burning, *Science*, 291, No. 5511, 2128-2132.
- (4) Pochanart P., J. Hirokawa, Y. Kajii, H. Akimoto and M. Nakao(1999): Influence of regional-scale anthropogenic activity in northeast Asia on seasonal variations of surface ozone and carbon monoxide observed at Oki Japan ,*J. Geophys. Res.*, 104, 3621-3631.
- (5) Japan Meteorological Agency(2002) : ANNUAL REPORT OF OZONE LAYER MONITORING:2001, pp.53.
- (6) Kim, Y.K., H.W. Lee, J.K. Park and Y.S. Moon(2002): The stratosphere-troposphere exchange of ozone and aerosols over Korea, *Atmospheric Environment*, 36, 449-463.

- (7) Kirchhoff, V.W.J.H., R.A. Baarnes and A. L. Torres(1991): Ozone climatology at Natal, Brazil, from in situ ozonesonde data, *J. Geophys. Res.*, 96, 10899-10909.
- (8) Cros, B., D. Nganga, A. Minga, J. Fishman and V. Brackett(1992):Distribution of tropospheric ozone at Brazzaville, Congo, determined from ozonesonde measurements, *J. Geophys. Res.*, 97, 12869-12875.
- (9) Crutzen P.J. and M.O. Andreae(1990): Biomass burning in the tropics: impact on atmospheric chemistry and biogeochemical cycles. *Science*, 250, 1669-1678.
- (10)Levine, J.S. (Editor), (1991): Global biomass burning: Atmospheric, Climatic, and Biospheric Implications, The MIT Press, Inc., 569.
- (11) Hudson R.D. and A.M. Thompson(1998): Tropical tropospheric ozone from total ozone mapping spectrometer by a modified residual method, *J. Geophys. Res.*, 103, 22129-22145.
- (12) Hayashida A.S., Sasano Y. And Iikura Y. (1991): Volcanic disturbance in the stratospheric aerosol layer over Tsukuba, Japan, observed by the National Institute For Environmental Studies Lidar from 1982 through 1986, *J. Geophys. Res.*, 96, 15469-15478.
- (13)Katamoto M., N.Furuhashi, I.Uno, S.Hayashida, R.Ide, M.Inagaki, M.Hashimoto, J.Zeng, H.Nakane and Y.Fujinuma(2002): Development of Air Mass Analysis system for Evaluating Tropospheric Monitoring Data Using ECMWF Upper Air Data-Calculation of Trajectory and Display of Meteorological Field-, Cger-Report, Cger-M013-2002, 111.
- (14) Heicklen J.(1976): Atmospheric chemistry, Academic Press, 274.

- (15) De Laat, A.T.J. and J. Lelieveld(2000): Diurnal ozone cycle in the tropical and subtropical marine boundary layer, *J. Geophys. Res.*, 105, 11547-11559.
- (16) Pochanart P., H. Akimoto, Y. Kinjo and H. Tanimoto(2002): Surface ozone at four remote island sites and the preliminary assessment of the exceedances of its critical level in Japan, *Atmospheric Environment*, 36, 4235-4250.
- (17) Fujiwara, M., K. Kita, T. Ogawa, S. Kawakami, T. Sano, N. Komala, S. Saraspriya and A. Suropto(2000):Seasonal variation of tropospheric ozone in Indonesia revealed by 5-year ground-based observations, *J. Geophys. Res.*, 105, 1879-1888.
- (18) Thompson, A.M., J.C Witte, S.J. Oltmans, F.J. Schmidlin, J.A. Logan, M. Fujiwara, V.W.J.H. Kirchhoff, F. Posny, G.J.R. Coetzee, B. Hoegger, S. Kawakami, T. Ogawa, J.P.F. Fortuin and H.M. Kelder(2003): Southern hemisphere additional ozonesondes (SHADOZ) 1998-2000 tropical ozone climatology 2. Tropospheric variability and the zonal wave-one, *J. Geophys. Res.*, 108, 8241-8256.
- (19) Monks P.S., G. Salisbury, G. Holland, S. A. Penkett and G. P. Ayers(2000) : A seasonal comparison of ozone photochemistry in the remote marine boundary layer, *Atmospheric Environment*, 34, 2547-2561.
- (20) Pochanart. P., J. Kreasuwun, P. Sukasem, W. Geeratihadaniyon, M.S. Tabulanon, J. Hirokawa, Y. Kajii, and H. Akimoto (2001): Tropical tropospheric ozone observed in Thailand, *Atmospheric Environment*, 35, 2657-2668.
- (21) Chan L.Y., H.Y. Liu, K.S. Lam, T. Wang, S.J. Oltmans and J.M. Harris (1998): Analysis of the seasonal behavior of tropospheric ozone at the Hong Kong, *Atmospheric Environment*, 32, 159-168.

- (22) Broennimann,S., E. Schuepbach, P. Zanis, B. Buchmann, H. Wanner(2000): A climatology of regional background ozone at different elevations in Switzerland (1992-1998), Atmospheric Environment, 34, 5191-5198.
- (23) Cooper S.M. and D.L. Peterson(2000): Tropospheric ozone distribution in western Washington, Environmental Pollution, 107, 339-347.

Chapter 5

Conclusion

In the first phase of this research, the suitable sampler for the on-board observation was developed. The sampler for the on-board observation was modified from a filtrating bulk sampler used widely in Japan. This sampler also fits the use in the remote forest, and the measurement accuracy using in the forest field was investigated.

The investigation on the collection method of rain and atmospheric depositions on board was conducted using three kinds of precipitation samplers. Type III of the precipitation sampler which has a slant opening of the upper funnel could collect rain and ion species most effectively. Type III sampler collected 3 to 4 times as much as the others in the precipitation. And Type III collected the ion species about twice as much as the others. Type III was the most suitable sampler for the rain measurement on board under high wind conditions.

In order to examine the chemical composition of atmospheric depositions in the remote marine areas, total 53 deposition samples were collected for 28 days from June 9 to July 6, 1999. They were measured on board of the R/V MIRAI of JAMSTEC. She devoted this measurement during the cruising of the international collaboration observation, the NAURU99 Experiment, in the Western Pacific Equatorial Ocean. The pH value of wet depositions ranged from 4.80 to 6.20 and was lower than pH 5 in three samples. The electric conductivity of wet depositions ranged from 2 to 2080 $\mu\text{S}/\text{cm}$.

Regarding both wet and dry atmospheric depositions, the ionic budget of the atmospheric deposition was satisfactorily balanced when the concentrations of nine major ions (H^+ , Na^+ , K^+ , NH_4^+ , Mg^{2+} , Ca^{2+} , SO_4^{2-} , NO_3^- , and Cl^-) were taken into account. Na^+ , K^+ , Mg^{2+} , Ca^{2+} , SO_4^{2-} , and Cl^- are the typical constituents of sea-salt particles, which form one part of atmospheric aerosols over the ocean, and the molar ratio shows good agreement to the ratio of seawater. The acidity of the atmospheric deposition was explained by the dilution of seawater. Winds cause a surge in the sea surface and generate sea-salt particles. The atmospheric deposition increases exponentially as the wind speed increases.

The investigation on wet and dry atmospheric depositions was carried out on board the T/S Nippon Maru, a tall sailing ship of the Independent Administrative Agency over the North Pacific Ocean. Although the main constituents of the atmospheric depositions originated from sea-salt constituents, the pH value of wet depositions was 4.1-6.8 and was lower than the pH of seawater. The atmospheric depositions in the mid-latitude seas of the westerly wind zone were acidified as strongly as they are in urban areas.

In this area, although there was no source of anthropogenic pollutants, $[\text{nss-SO}_4^{2-}]$ and $[\text{NO}_3^-]$ in the atmospheric depositions were higher than they were in the lower latitudes of the trade-wind zone. These constituents were generally considered to have originated in East Asia. However, we were not able to determine any tendency in attenuation relative to the distance from Japan. However, in the low latitudes of the sea in the trade-wind zone, the constituent concentrations of the atmospheric depositions were low, and they changed very little.

$[\text{H}^+]$ in diluted seawater was calculated theoretically and compared with the measured $[\text{H}^+]$. The difference was related to the ion balance of the nss-constituents.

We concluded that nss-SO_4^{2-} and NO_3^- were acidification constituents and that nss-cations were neutralization constituents.

Ozone plays an important role in global environment formation by shutting off harmful ultraviolet rays, by giving effect on global warming or by acidifying atmospheric deposition. In recent years, increase of tropospheric ozone concentration has been pointed out. To obtain the distribution and the trend of tropospheric ozone in the western Pacific zone, the atmospheric ozone concentration was monitored during one-month cruising between Japan and Australia every August from 1993 to 1998 and from January 23rd to March 2nd in 1998. The results were shown as follows.

The concentration measured on the sea was constant and no diurnal variations caused by photochemistry as seen in the urban areas were observed. In summer cruise, the ozone concentration in 30 degrees N was about 12ppbv and exhibited an increasing trend toward to the equator in the northern hemisphere, where the concentration was about 19ppbv. In the southern hemisphere, the similar trend was observed and the concentration increased with increasing the latitude. The concentration marked almost 27ppbv in 30 degrees S. In winter, the ozone concentration increased contrary to that observed in summer. The concentration was about 47ppbv in 30 degrees N, decreased to about 22ppbv on the equator and further decreased to about 11ppbv in 20 degrees S.

In our research area, northerly and southerly winds blew in winter and summer respectively. The meridional distribution of the ozone concentration was depending on the change of the general wind direction. The ozone concentration decreased leeward along general wind.

To study the route of the air mass, back trajectory analysis of the measured air mass was performed. The initial altitude of the back trajectory was 1200m and the air

mass history was traced for 5 days. The maximum passing altitude was 6000m. It was found out that the ozone concentration of the air mass was well proportional to the maximum passing altitude of the air mass trajectory.

Acknowledgments

The author wishes to express his greatly heartfelt appreciation to all people who provided his invaluable helps and encouragements during the present study from 1998 to 2003 at Maritime University of Kobe.

First of all, he wishes to express his sincere and heartfelt gratitude to his supervisor, Prof. Dr. Hiroshi Ishida of Maritime University of Kobe, for his incessant inspiration, continuously encouragement, suitable guidance and patient education throughout this study. The author is greatly indebted to Profs. of Maritime University of Kobe, Drs. Shinichi Nagata, Keiichi Fukushi and Haruo Mimura who offered a number of suggestions for this study. He also thanks sincerely to coauthors, Dr. T. Tamaki, Mr. M. shoga, and Drs. M. Aikawa, T. Kobayashi, and Y.Nakagawa of Hyogo Prefectural Institute of Public Health and Environmental Sciences and Dr. M.Hayashi of Maritime University of Kobe.

The author would like to express his greatly heartfelt appreciation to all the staff of Hyogo Joint Summer Session at Sea and the captain and his crew of the P/V Orient Venus of Japanese Cruise Line Co., Ltd. for their wonderful arrangements and heartfelt cooperation. Thanks also are expressed to the chief scientist, Dr. Yoneyama of the Japan Marine Science and Technology Center (JAMSTEC), the captain of the R/V MIRAI, Dr. Akamine and his crew for their wonderful cooperation during the experiment in the Western Pacific equatorial Ocean.

The author also thanks to Captain Nakamura and the crew of the T/S Nippon Maru and Captain Ikeda and his crew of the T/S Hokuto Maru of the National Institute for Sea Training, Independent Administrative Institution of Japan, and Mr. Iwao, a graduate

student of Maritime University of Kobe, for their assistance. He also expresses his most sincere gratitude to the members of the department of investigation and research of the National Institute for Sea Training for the excellent arrangements they made for this research.

He also wants to thank the staffs of Center for global Environmental Research of National Institute for Environmental Studies for their wonderful supports on air mass back trajectory analysis and especially to Dr. Katsumoto Masayuki for giving his suitable guidance and cooperation.

Papers Published and Submitted

1. Hiraki T., H.Ishida and M.Hayashi: Measurement of the Atmospheric Deposition over the Western Pacific Equatorial Ocean, The Marine Meteorological Society, Sea and Sky(海洋気象学会、海と空), Vol.76, No.2, 119-124, 2000. (Chapter 2)
2. Tamaki M., T.Hiraki, Y.Nakagawa, T.Kobayashi, M.Aikawa and M.Shoga: Study on Sampling Method of Rainfall, Throughfall and Stemflow Concerning with Acid Deposition Effect on Forest Ecosystem, Water, Air and Soil Pollution, Vol.130, 1511-1516, 2001. (Chapter 1)
3. Hiraki T., M.Aikawa, M.Tamaki, M.Shoga and H.Ishida : Characteristics of Atmospheric Depositions over the North Pacific Ocean, The Marine Meteorological Society, Sea and Sky(海洋気象学会、海と空), Vol.77, No.3,135-140, 2001. (Chapter 3)
4. Hiraki T., M.Tamaki, M.Shoga and H.Ishida : Improvement of the Precipitation Sampling Method on Board, Proceedings of the International TECHNO-OCEAN 2002, pp5 (various page), 2002. (Chapter 1)
5. Hiraki T., M.Tamaki, M.Aikawa and H.Ishida : Seasonal variation of Ozone Concentration in the Atmosphere over the Western Pacific Ocean, The Marine Meteorological Society, Sea and Sky(海洋気象学会、海と空), Vol.79, No.3, in press, 2003. (in Japanese). (Chapter 4)